FINAL PROJECT REPORT

SELF-CORRECTING CONTROLS FOR VAV SYSTEM FAULTS

Filter/Fan/Coil and VAV Box Sectons

Prepared for CIEE By:

Pacific Northwest National Laboratory

Project Manager: Michael R. Brambley

Authors: Michael R. Brambley, Nick Fernandez, Weimin Wang, Katherine A. Cort, Heejin Cho, Hung Ngo, James Goddard

Date: May, 2011

A CIEE Report

PREFACE

This report documents work performed by Pacific Northwest National Laboratory for the California Institute for Energy Efficiency under subcontract PODR01-X08 between The Regents of the University of California and Battelle, Acting on behalf of Pacific Northwest National Laboratory.

ABSTRACT

This report documents original research by the Pacific Northwest National Laboratory (PNNL) for the California Institute for Energy and Environment on self-correcting controls for variable-air-volume (VAV) heating, ventilating and air-conditioning (HVAC) systems and focuses specifically on air handling and VAV box components of the air side of the system. A complete set of faults for these components was compiled and a fault mode analysis was performed to understand the detectable symptoms of the faults and the chain of causation. A set of 26 algorithms was developed to facilitate the automatic correction of these faults in typical commercial VAV systems. These algorithms include training tests that are used during commissioning to develop models of normal system operation, passive diagnostics used to detect the symptoms of faults, proactive diagnostics used to diagnose the cause of a fault, and fault correction algorithms. Of the 26 algorithms, 10 were implemented in a prototype software package that interfaces with a test bed facility at PNNL's Richland, WA, laboratory. Measurement bias faults were instigated in the supply-air temperature sensor and the supply-air flow meter to test the algorithms developed. The algorithms, as implemented in the laboratory software, correctly detected, diagnosed and corrected faults in most cases tested. An economic and impact assessment was performed for deployment of self-correcting controls in California. Assuming 15% HVAC energy savings and a modeled deployment profile, 3.1 TBtu to 5.8 TBtu of energy savings are possible by year 15 of deployment.

Keywords: California Energy Commission, PNNL, self-correcting controls, VAV, faults, fault detection and diagnosis

Please use the following citation for this report:

Brambley, Michael R., Nick Fernandez, Weimin Wang, Heejin Cho, Hung Ngo and James Goddard. (Pacific Northwest National Laboratory) 2011. ***Self-Correcting Controls for VAV System Faults – Filter/Fan/Coil and VAV Box Sections***.

TABLE OF CONTENTS

EXECUTIVE SUMMARY

The Pacific Northwest National Laboratory (PNNL) performed research for the California Institute for Energy and Environment (CIEE) in self-correcting controls for commercial building VAV systems. The work included identification and analysis of fault modes and their symptoms, developing algorithms for the four steps of the process leading to automated correction of faults not requiring human intervention to physically repair or replace a system component, coding a selected subset of the algorithms in prototype laboratory-grade software, and laboratory testing. These steps in the process include training to capture relationships among key variables, fault detection, fault diagnosis (which is also known as fault isolation), and fault correction. The remainder of this executive summary briefly describes the work performed and key results and is organized in parallel to the chapter structure of the report.

Identify Faults

A comprehensive list of faults that affect VAV systems was developed and mapped to their potential causes to facilitate the development of algorithms. The list of faults was developed in a brainstorming session that brought together several experts with experience in diagnosing faults in HVAC systems and developing automated HVAC control and fault detection and diagnostic (FDD) systems. The faults were categorized as hard (physical) or soft (software) component faults. The components for which faults were identified include temperature, pressure, and air-flow rate sensors, valves, dampers, fans, filters, coils, economizers, VAV boxes, and supply-fan controls. Through a process called fault mode analysis, these faults were mapped to observable symptoms, which are indicators of deviations from expected system behavior. Some of these symptoms are easily observable (for example, if the measured supply-air temperature is colder than the mixed-air temperature when the coiling-cool valve in an air-handler has been commanded closed.) Other faults require the development of more complex models to empirically define normal operating conditions.

A total of 28 faults were identified that can be diagnosed in the air-handler (filter/fan/coil) and VAV-box sections of the air side of VAV systems in this set of algorithms. Of these, 18 are automatically correctable soft faults, and 10 are hard faults that require physical repair or replacement.

Development of Self-correction Methods and Algorithms

Based on physical principles, equipment design, and the insights gained from the fault-mode analysis, a set of rule-based algorithms was developed to facilitate automatic correction of the identified faults. The structure for these algorithms is the same structure used previously by PNNL in development of self-correcting controls for the mixing-box section of air handlers. This structure is a four-step process to fault correction. The first step, training, establishes the normal range for a set of variables and quantitative empirical relationships among some for later use in fault detection and diagnosis. The next step, passive fault detection (or passive diagnostics) uses observation of fault symptoms during ordinary operation to detect when a fault has occurred. After a fault is detected, proactive diagnostics (tests) are used to isolate

which of potentially several possible faults was responsible for the observed symptom. This typically requires more information than is available from normal operation of the system, so specific diagnostic tests are run to create situations that provide additional data and information. After the fault has been isolated, the fault correction process characterizes the fault (e.g., the magnitude of a constant bias in a sensor output rather than erratic, constantly changing, sensor output), formulates a mathematical description of the fault, and then subtracts the fault to compensate the behavior of the faulty device. The correction is implemented via a virtual point (e.g., sensor output, control signal, etc.). The algorithms are documented in detail in a companion report identified in the reference list of this report as Fernandez et al. 2011.

Implementation of Algorithms in Software Code and Integration with the Control System

The algorithms were successfully coded in prototype software using the Jython programming language (a hybrid of Java and Python). A subset of the full suite of algorithms was coded. Priority was given to the development of all four steps of the fault-correction process for two key soft faults: biased supply-air flow-rate sensors and biased supply-air temperature sensors. The software was integrated with a Johnson Metasys Building Automation System, using Factory Plant Management Interface (FPMI) software. The software uses two sets of virtual points for sensors. The first enables simulation of sensor faults through virtual sensor points that the control system reads in lieu of the direct sensor measurements. These virtual sensor points enable instigation of faults without damaging equipment and the outputs of these virtual sensors exhibit the characteristics of the fault of interest. The other virtual sensor points enable application of corrections developed by the self-correcting algorithms to the faulty sensor signals to create corrected sensor signals that replace erroneous values to the control algorithms.

Laboratory Testing of the Self-Correcting Software

Six laboratory tests were performed. Three tests of supply-air flow-rate sensor bias and three tests of biased supply-air temperature sensors were performed. The three tests for each fault were used to investigate differences in the outcome of the test as functions of fault severity and the values of key selectable thresholds for fault detection. The tests were each initiated with a 5-minute period of fault-free operation, during which no faults were detected. In all tests, the passive diagnostic tests successfully detected a fault soon after its instigation. In four tests, the fault was correctly diagnosed, and automatically corrected approximately to the level of the instigated bias. Faults with low severity and higher detection thresholds presented problems, which led to an inconclusive result for one test of the biased supply-air temperature sensor and an incorrect fault determination for one test for the biased supply-air flow-rate sensor. Modest changes in the algorithms are proposed to account for these issues. All methods for fault detection and diagnosis impose a tradeoff between sensitivity and false positive fault detection. Generally, as sensitivity is increased, the probability of false positives increases. Therefore, achieving the right balance between these behaviors is critical to successful deployment of the technology. Further laboratory testing will be used to "tune" the associated variables (e.g., detection thresholds and sensor tolerances).

Economic and Impact Assessment of Deployment

The targeted market for self-correcting controls in the short-term is built-up air systems, with a longer-term target of packaged HVAC systems. The benefits for self-correcting controls are estimated with PNNL's Building Energy Analysis Modeling System (BEAMS) using data for California. The market penetration over time is developed based on market diffusion curves, which are based on the Bass diffusion model. The analysis estimates 1.2 to 2.4 TBtu in annual energy savings for the State of California from built-up systems by the end of year 15 after commercial introduction to the market and 1.9 to 3.8 TBtu by the end of 15 years for packaged systems (but with a lower initial impact than built-up systems). Combining the two targeted markets, potential annual savings equal up to $160 million by year 15 with corresponding reductions in CO_2 emissions of 130,000 metric tons.

The Path Forward

The final chapter of the report identifies specific proposed improvements to the algorithms to improve their performance, including:

- Piecewise empirical models to capture relationship between variables better when distinctly different behavior exist (e.g., a range of control commands for which no measurable response occurs compared to a range where the response monotonically increases with increasing control command).

- Use of cooling-coil effectiveness as the basis for relating the temperature change or air as it passes across the cooling coil to supply-fan speed and control signal to the chilled-water valve.

Additional laboratory testing of the full suite of algorithms to better understand preferred values for selectable parameters (e.g., detection thresholds), to ensure that the algorithms minimize false fault detection, and prepare the full suite of self-correcting algorithms for VAV systems for field application.

The collective findings of the PNNL team in this project and prior work support development of a software module for self-correcting air-handler sensors, which would be suitable for use in field tests and early commercialization. Although the caabilities of this module would be limited in scope, they would address the important problems of out-of-calibration sensors in air-handling systems.

CHAPTER 1:
Fault Identification and Analysis

This chapter includes three sections. In the first section, the typical single-duct variable-air-volume (VAV) air-handling unit (AHU) and the VAV terminal boxes are briefly described, along with operating modes and sequences of control. Potential faults are presented in the second section for each component of the VAV system, and in the third section, a number of cause-effect diagrams are used to associate fault symptoms to the faults themselves, which are identified in the second section.

System Description

The single-duct, VAV air-handling and distribution system is described in this section with the AHU and VAV terminal boxes described separately. The AHU receives return air from the building zones, recirculates a fraction of it and exhausts the rest to the outdoors. The recirculated air mixes with outdoor air in the mixing box. The mixed air is then filtered, cooled (or heated), and then distributed to the terminal boxes, which further control the air-flow to each zone and reheat the supply-air, if necessary.

Air-handling Unit (AHU)

Figure 1 is a schematic diagram of a generic single-duct AHU for VAV systems. Typical sensors are identified by labeled, colored circles (see the key in the lower-right in the figure).

Figure 1: Diagram of a Typical VAV Air-handling Unit

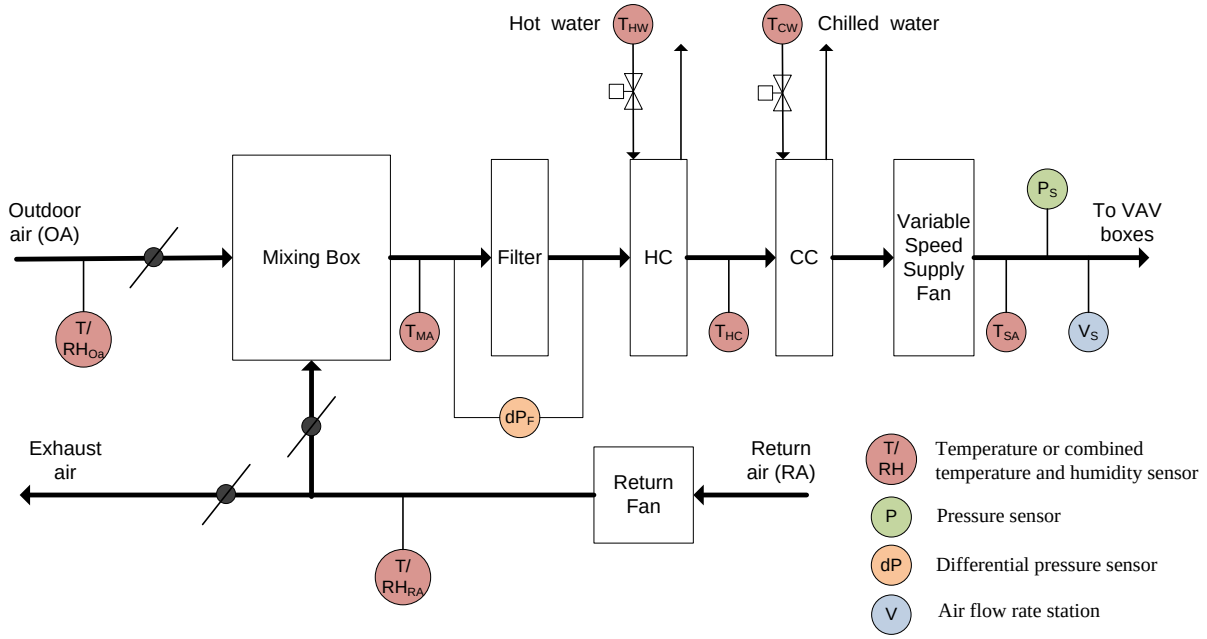

Outdoor air (OA) enters the AHU, passing through the outdoor-air damper, and is mixed with the air returned from the space via a return fan. The mixed air sequentially passes through the

filter, the heating coil (HC), if present, and the cooling coil (CC), which are used to maintain the supply-air at a predefined temperature set point in the supply duct downstream of the supply fan. In practice, the supply fan may be located either upstream of the coils (blow through) or downstream of the coils (draw through, as shown in Figure 1). In many systems, only a cooling coil is present. The supply-fan speed is modulated to maintain the supply-air static pressure at a set point. The return-fan speed is set according to the building's pressurization requirement and the speed of the supply fan.

When the AHU is in operation during occupied periods, it may work in one of four operating modes: heating with minimum outdoor OA, economizing (with OA used for cooling), mechanical cooling with full economizing (100% OA), and mechanical cooling with minimum OA. The specific mode used depends on the outdoor-air conditions. The modes are shown graphically in Figure 2 and are described below.

Figure 2: Air Handler Operating Modes

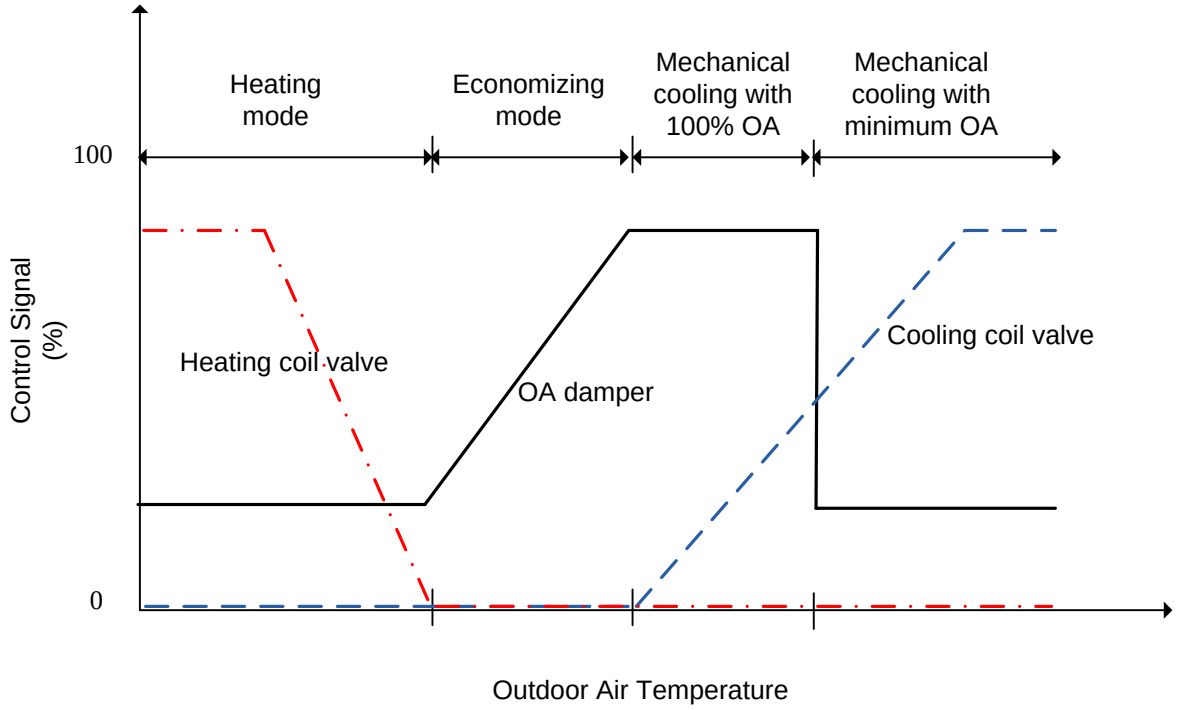

Heating mode

In this mode, the OA temperature is low enough that the mixed-air (MA) temperature is lower than the supply-air temperature set point, even if the OA damper is at the minimum position required to meet ventilation requirements. Thus, the heating coil valve is controlled to an open position to heat the supply air to its set point, while the cooling coil valve is fully closed, and the OA damper is kept at its minimum position.

Economizing (OA cooling) mode

At higher OA temperatures, the AHU changes from the heating mode to cooling with OA (i.e., economizing with no mechanical cooling). In this mode, both the heating-coil and the cooling-coil valves are closed and the supply-air temperature is maintained at its set point by modulating the mixing-box dampers (opening the outdoor-air damper and closing the return-air damper as the need for cooling increases).[1]

Mechanical cooling with full economizing (100% OA mode)

As the cooling load continues to increase, the OA damper opens until it reaches its maximum open position, provided the OA temperature (or enthalpy) remains sufficiently low to provide cooling. If economizing with 100% OA cannot lower the MA temperature to the supply-air set point, mechanical cooling is initiated by modulating the cooling-coil valve open sufficiently to lower the supply-air temperature to its set point to meet the load that economizing cannot meet. This mode of economizing is frequently referred to as integrated. The heating coil valve is kept completely closed in this operating mode. Some economizer controls, known as non-integrated, do not simultaneously use economizing and mechanical cooling. These systems do not enter the mechanical cooling with full economizing mode.

Mechanical cooling with minimum OA mode

When the OA temperature (or enthalpy) increases above the return-air temperature (or enthalpy) or other pre-specified limit, the OA damper modulates back to its minimum position for ventilation, and mechanical cooling is used to meet the entire cooling load. The cooling coil valve is modulated to provide the required mechanical cooling, while the heating coil valve is kept completely closed.

Variable-air-volume (VAV) Terminal Boxes

VAV boxes are an integrated part of the VAV system. In contrast to the air-handling unit, VAV terminal units have more varied types such as fan-powered terminal units, induction terminal units, and throttling VAV terminal units with or without reheating. In the current stage of this project, the fault analysis focuses on the single-duct, pressure-independent throttling VAV box with hydronic reheat as shown in Figure 3. This box captures many of the features of simpler terminal boxes, which can be modeled by deleting features of this box (e.g., terminal reheat). For the VAV box shown in Figure 3, the controller modulates the damper to meet thermal load requirements. A minimum air flow rate is preset to satisfy space ventilation. The valve can modulate the hot-water flow rate to the reheat coil to raise the temperature of the supply air to moderate cooling or to provide heat to the space.

These VAV terminal boxes work in one of three operating modes: cooling with more than the minimum air flow rate, deadband mode, and reheating. The specific mode of operation

[1] Economizing may be controlled on dry-bulb temperature or enthalpy.

Figure 3: Schematic diagram of a pressure-independent VAV box with hydronic reheat. Solids lines represent flows of air and water; dashed lines represent control connections.

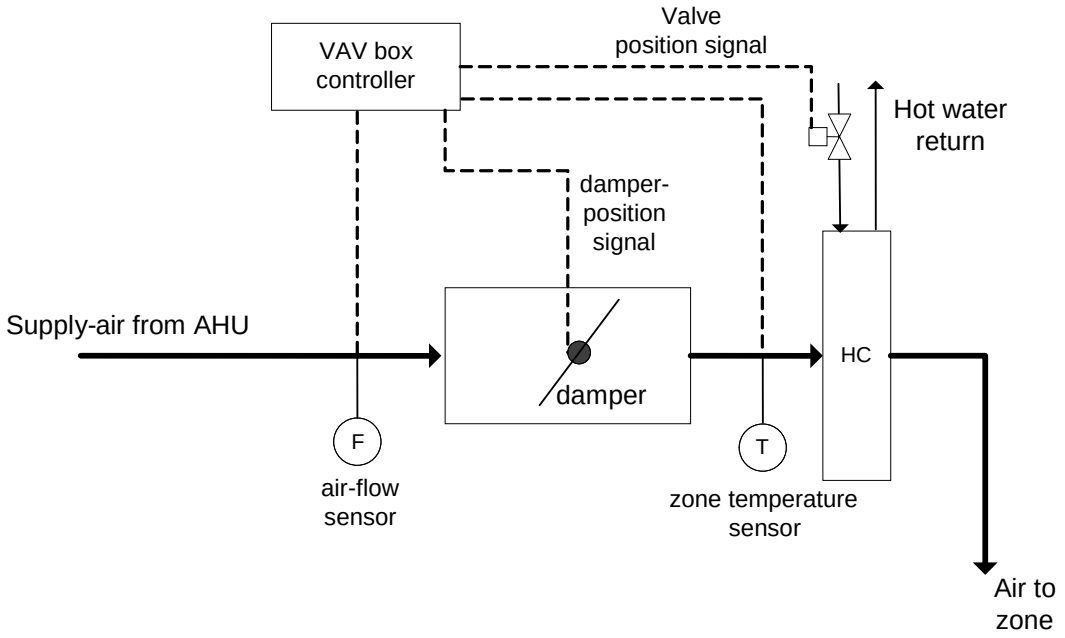

Figure 4: Operating modes for a single-duct, pressure-independent throttling VAV box with hydronic reheat

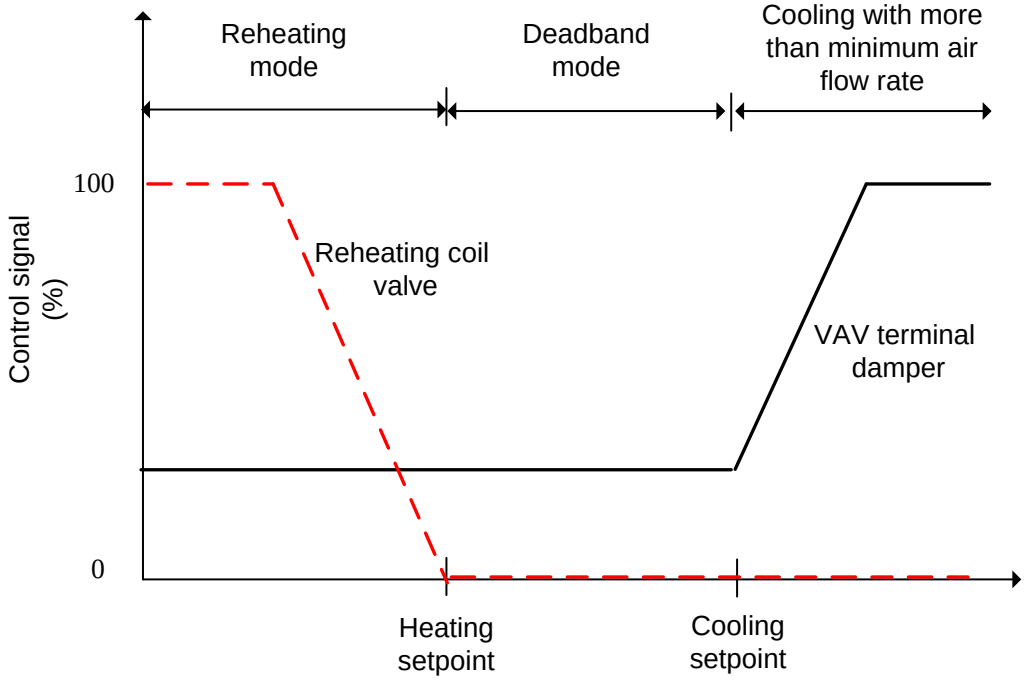

depends on the zone-air temperature. The operating modes are shown graphically in Figure 4 and are described below.

Cooling with more than the minimum air flow rate

The VAV box operates in this mode when the zone-air temperature increases above the space cooling set point. In this case, the air flow rate is increased by increasing the damper opening. The reheat coil valve is kept closed.

Deadband mode

The VAV box operates in this mode when the zone-air temperature lies between the space cooling and heating set points. The air flow rate is maintained at the minimum value to meet the ventilation requirement, and the reheat coil valve is kept closed.

Reheating

The VAV box enters this mode when the zone-air temperature decreases below the space heating set point. In this case, the valve for the reheat coil modulates to meet the space heating load. The air flow rate may be kept constant at its minimum value or the VAV damper may open further to meet additional space heating load after the reheat valve has opened 100%.

Identification of potential faults

Potential faults in air-handling units and the associated VAV terminal boxes can be identified in two steps. First, a preliminary list of potential faults was prepared based on review of the literature on fault detection and diagnostics (FDD) for AHUs and VAV boxes (see, e.g., Fernandez et al. 2009a; Fernandez et al. 2009b; Dexter and Pakanen 2001; Hyvarinen and Karki 1996; Smith and Bushby 2003). The literature has generally focused on detection and diagnosis for a number of common faults (e.g., sensor biases and control logic errors). Little attention has been given to developing a comprehensive list of potential faults and the causes of those faults. Therefore, a second step was used to address this limitation and identify a more complete set of faults and their potential causes. A group of eight researchers identified and discussed additional faults and underlying causes observed in the field to develop a complete set of symptoms, faults and underlying causes. The field experience of each participant in HVAC system implementation, maintenance and troubleshooting varied from approximately 2 years to over 30 years.

HVAC faults can be classified into different categories according to criteria such as complete component failure versus performance degradation, hardware faults versus software faults, and self-correctable faults versus faults requiring human corrective action. Because this work is performed in the context of self-correcting HVAC control, each fault is categorized as self-correctable (SC), possibly self-correctable (PSC), and not self-correctable (NSC). A SC fault is one that can be corrected through changes in the values of parameters or to software code in the control system. These faults include, for example, incorrect schedules, poorly chosen set points, continually oscillating (or hunting) controls, incorrectly implemented controls, and failed or out-of-calibration sensors. A PSC fault is one for which self correction may be feasible under certain circumstances, one for which the team is presently uncertain that self correction can be implemented, or a fault that may be correctable if additional sensors were installed beyond

those ordinarily present on the HVAC system. An NSC fault is one for which restoration to normal system performance from the faulty situation is not possible without physical repair of the system, which requires human intervention.[2]

The potential faults for the VAV air-handling system described earlier in this chapter are identified in Table 1 through Table 4. Each table presents the faults for one of the major parts comprising the VAV system: air-mixing section, filter-coil section, fan section, and VAV boxes. The categorization of each fault is given in the right-most column of each table, using the abbreviations SC, PSC and NSC.

[2] NSC faults generally result from physical failure of components, but all physical faults are not NSC faults. In fact, as stated in the text, some physical faults, such as complete failure of some sensors, can be automatically corrected. Furthermore, compensation for some physical faults that improves performance of the system above the performance that would occur by default when a physical fault or failure occurs may be possible. Such fault compensation will be considered in future research.

Table 1: Air-Mixing Section Faults

Components	Type of Fault/Failure	Specific Fault	Fault Category (SC, PSC or NSC)*
Temperature or humidity sensors (return air—RA, outdoor air—OA, mixed-air—MA)	Complete failure—no signal		SC
	Constant bias in signal	Sensor out of calibration	SC
		Sensor installation location fault	PSC
		Wiring fault	SC
		Long lead wires	SC
	Time varying bias in signal	Sensor installation of location fault	PSC
		Drifting signal	SC
	Intermittent signal	Communication problems such as a wiring fault	PSC
		Sensor internal fault	PSC
		Wiring fault (e.g., bad solder joint)	PSC
	Randomly varying signal	Communication problems such as a wiring fault	PSC
		Sensor internal fault	PSC
		Induced electrical noise	PSC
Damper and actuator	Stuck damper (fully open, completely closed, intermediate position)	Damper motor failure	NSC
		Damper linkage broken or disconnected	NSC
		Damper or linkage stuck from rust or other corrosion	NSC
		Wire to actuator disconnected or no power	NSC
		Controller in manual mode	PSC
	Air leakage when damper is fully closed	Damper blade damaged	NSC
		Poor damper seals	NSC
		Damper not closing completely	PSC

	Damper modulating but too open or too closed	Damper obstructed	NSC
		Damper linkage bent or loose	NSC
		Incorrect actuator output range	PSC
		Damper behavior not properly calibrated	SC
Mixed-air controller (economizer and outdoor-air ventilation control)	No control signal	Wire disconnected	NSC
		Sensor failure	PSC
		Control card failure	PSC
	Controller in manual mode		PSC
	Incorrect minimum outdoor-air damper position setting in control code		SC
	Dampers hunting	Improperly tuned control parameters	SC
	Actuator output range not set correctly		SC
	Error in control code (logic)		SC
	Incorrect or poor economizer control	Poorly chosen values for control parameters	SC
		Error in coding of economizer control sequence	SC
	Fault in CO_2 sensor for demand control ventilation (see “Temperature or humidity sensor faults” for possible causes)		PSC

* SC = self correctable; PSC = possibly self correctable; NSC = not self correctable.

Table 2: Filter-coil Section Faults

Components	Type of Fault/Failure	Specific Fault	Fault Category (SC, PSC or NSC)*
Temperature or humidity sensors (return air—RA, outdoor air—OA, mixed-air—MA)	Complete failure—no signal		SC
	Constant bias in signal	Sensor out of calibration	SC
		Sensor installation location fault	PSC
		Wiring fault	SC
		Long lead wires	SC
	Time varying bias in signal	Sensor installation location fault	PSC
		Drifting signal	SC
	Intermittent signal	Communication problems such as a wiring fault	PSC
		Sensor internal fault	PSC
		Wiring fault (e.g., bad solder joint)	PSC
	Randomly varying signal	Communication problems such as a wiring fault	PSC
		Sensor internal fault	PSC
		Induced electric noise	PSC
Damper and actuator	Stuck damper (fully open, completely closed, intermediate position)	Damper motor failure	NSC
		Damper linkage broken or disconnected	NSC
		Damper or linkage stuck from rust or other corrosion	NSC
		Wire to actuator disconnected or no power	NSC
		Controller in manual mode	PSC
	Air leakage when damper is fully closed	Damper blade damaged	NSC
		Poor damper seals	NSC
		Damper not closing completely	PSC

	Damper modulating but too open or too closed	Damper obstructed	NSC
		Damper linkage bent or loose	NSC
		Incorrect actuator output range	PSC
		Damper behavior not properly calibrated	SC
Mixed-air controller (economizer and outdoor-air ventilation control)	No control signal	Wire disconnected	NSC
		Sensor failure	PSC
		Control card failure	PSC
	Controller in manual mode		PSC
	Incorrect minimum outdoor-air damper position setting in control code		SC
	Dampers hunting	Improperly tuned control parameters	SC
	Actuator output range incorrectly set		SC
	Error in control code (logic)		SC
	Incorrect or poor economizer control	Poorly chosen values for control parameters	SC
		Error in coding of economizer control sequence	SC
	Fault in CO_2 sensor for demand control ventilation (see "Temperature or humidity sensor faults" for possible causes)		PSC

* SC = self correctable; PSC = possibly self correctable; NSC = not self correctable.

Table 3: Fan Section Faults

Components	Type of Fault/Failure	Specific Fault	Fault Category (SC, PSC or NSC)*
Fan (supply fan-SF, return fan-RF)	Complete failure	Power disconnected	NSC
		Blown fuse	NSC
	Off for protection (design safety measures)		NSC
	Decrease in fan efficiency	Dirt accumulation	NSC
		Loose fan blade	NSC
		Other efficiency degradation	NSC
Pressure sensor (supply-air duct; see "Temperature or humidity sensor faults" in Table 1 for detailed fault or causes)	Complete failure		PSC
	Biased signal		PSC
	Drifting signal		PSC
	Intermittent signal		PSC
	Randomly varying signal		PSC
Supply and return fan controller	No control signal	Wire disconnected	NSC
		Sensor failure	PSC
		Controller card failure	NSC
	Improperly tuned control parameters		SC
	Improper set point for supply-air duct pressure		SC
	Controller software and parameter value faults	Improper value for supply-air temperature set point	SC
		Error in control code (logic)	SC
	Actuator output range not set correctly		SC
	Inappropriate override of automatic operation (e.g., variable flow rate bypass mode on)		SC

* SC = self correctable; PSC = possibly self correctable; NSC = not self correctable.

Table 4: VAV Terminal Section Faults

Components	Type of Fault/Failure	Specific Fault	Fault Category (SC, PSC or NSC)*
Damper and actuator	Stuck damper (fully open, completely closed, or intermediate position)	Damper motor not working	NSC
		Damper linkage broken	NSC
		Damper or linkage frozen from rust or other corrosion	NSC
		Wire to actuator disconnected or no electrical power	NSC
	Incorrect minimum or maximum flow rate set point		SC
	Damper not fully open at maximum position	Damper physically obstructed	NSC
		Damper linkage bent or loose	NSC
		Incorrect actuator output range	SC
Air-flow sensor (see "Temperature or humidity sensor fault" in Table 1 for detailed specific causes or faults)	Complete failure		PSC
	Biased signal		PSC
	Drifting signal		PSC
	Intermittent signal		PSC
	Randomly varying signal		PSC
Reheat coil	Poor heat transfer from fouling (air or water side)		NSC
	Wrong coil capacity (oversized or undersized)	Design fault	NSC
		Change in space function or usage pattern	NSC
	Water leakage from coil		NSC
	Reduced water flow rate caused by water-side balance problems		NSC
Valve and actuator (for reheat coil)	Valve stuck (fully open, completely closed, or intermediate position)		NSC
	Water leakage when valve in closed		NSC
	Flow blocked		NSC
	Valve sized improperly		NSC

	Valve modulating but not fully opening or closing (not modulating over full range)		PSC
Zone-temperature sensor (see "Temperature or humidity sensor fault" in Table 1 for detailed specific causes or faults)	Complete failure		PSC
	Biased signal		PSC
	Drifting signal		PSC
	Intermittent signal		PSC
	Randomly varying signal		PSC
VAV box controller	No control signal	Wire disconnected	NSC
		Sensor failure	PSC
		Controller-card failure	NSC
	Controller in manual mode		PSC
	Improperly tuned control parameters		SC
	Controller software fault	Improper value for zone-air temperature set point	SC
		Error in control code	SC
	Actuator output range not set correctly		SC

*SC = self correctable; PSC = possibly self correctable; NSC = not self correctable.

Fault mode analysis

Different faults may lead to the same symptom, such as an unmet supply-air temperature set point or increased heating energy use. A clear structured relationship between the HVAC faults presented in the last section and their manifested symptoms will assist in developing the strategies for fault detection, isolation and self-correction presented later in this report.

We use cause and effect diagrams (also known as fishbone or Ishikawa diagrams) as the tool to explore and document all potential causes (or faults) that result in a single effect (or symptom). Faults (and/or causes of faults) are arranged according to their level of detail or position in the chain of causality. Thus, a significant advantage of this diagram is its ability to clearly illustrate the hierarchical relationship between a specific outcome and the factors that influence or can lead to that outcome. A generic version of the cause and effect diagram is shown in Figure 5.

Consider Figure 6 as an example. The symptom (i.e., effect) is an incorrect value from a sensor, which may be caused by a biased signal, a drifting signal, a randomly varying signal, an intermittent signal, or no signal. Each of these causes can be further analyzed to explore underlying causes.

Figure 5: Generic Cause and Effect Diagram Adapted for Application to Equipment Faults

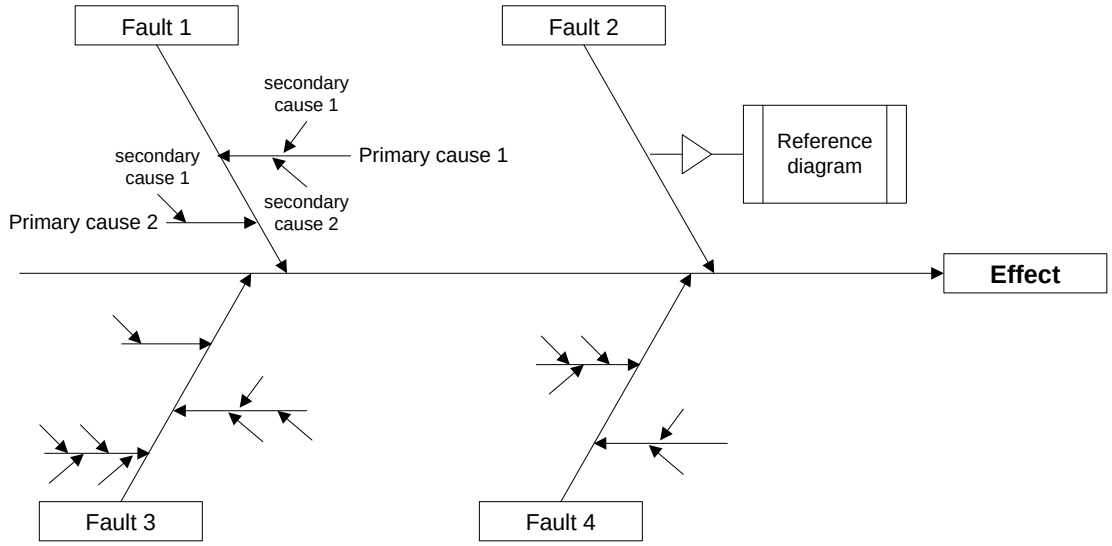

Figure 6: Cause-effect Diagram for an Incorrect Sensor Measurement

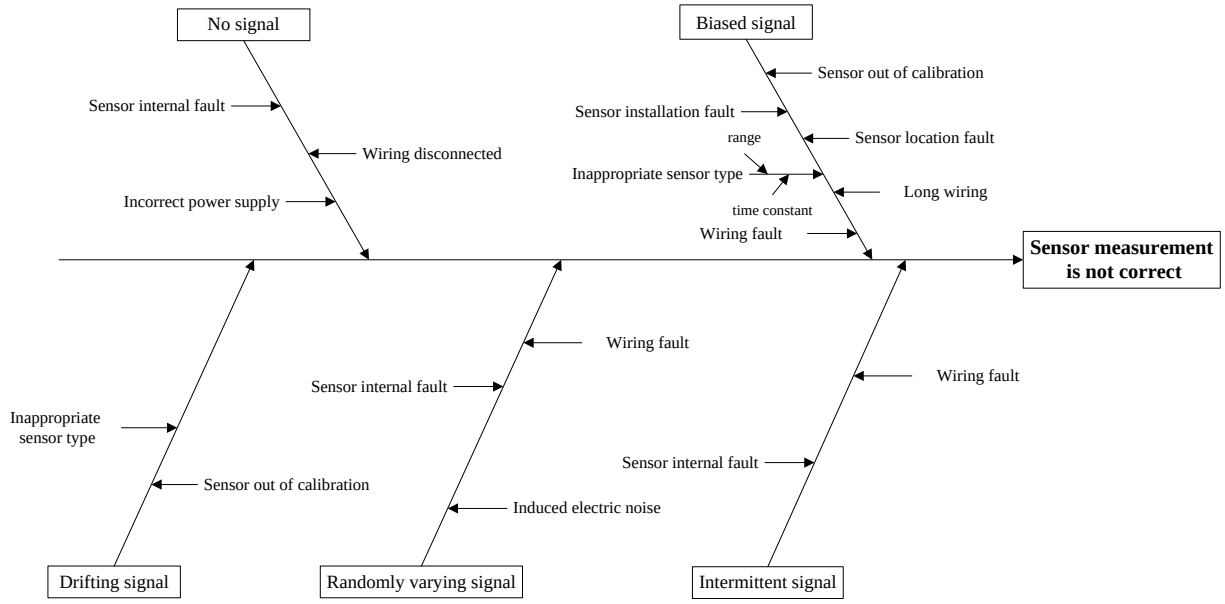

Because an HVAC symptom is an observed deviation from normal (or expected) operation, it is convenient to select the directly measured variables, control signals and easily derived variables as indicators of symptoms. Cause-effect diagrams are presented for a total of 11 symptoms (effects) in Figure 6 through Figure 16. The symptoms for which cause-effect diagrams are shown are:

- Sensor measurement is not correct
- MA temperature differs from normal values under similar operating conditions

- Supply-air temperature differs from its set point
- Supply-air pressure differs from its set point
- AHU operation mode changes more frequently than normal
- Supply-air flow rate differs from normal values under similar operating conditions
- Supply-fan energy use differs from normal values under similar operating conditions
- AHU heating energy use differs from normal values under similar operating conditions
- AHU cooling energy use differs from normal values under similar operating conditions
- Zone-air temperature differs from its set point
- VAV box flow rate differs from normal values under similar operating conditions.

Cross references to fault analyses for different symptoms are used in Figure 6 through Figure 16 to make the cause-effect diagrams clearer and more legible. For example, Figure 7 refers to Figure 6 regarding the possible faults for temperature sensors, humidity sensors and CO_2 sensors.

The cause-effect diagrams are tools used for formulating algorithms for self correction of amenable faults in air handlers and VAV terminal boxes in Chapter 2.

Figure 7: Cause-effect Diagram for the Mixed-air Temperature Differing from Values Normally Occurring Under Similar Operating Conditions

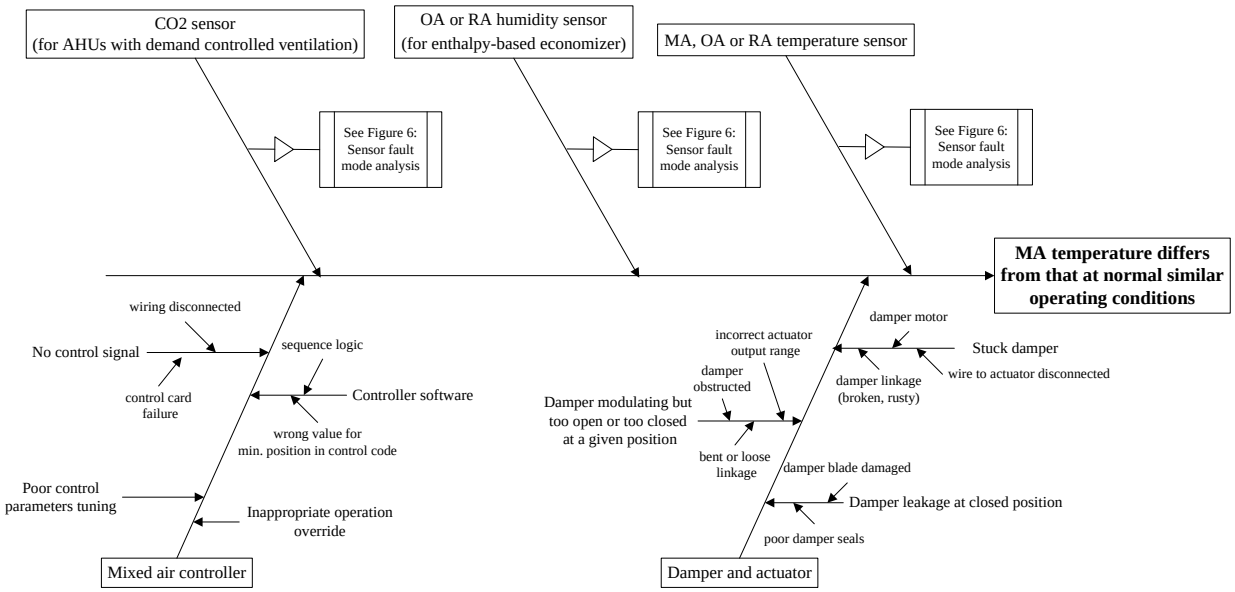

Figure 8: Cause-effect Diagram for the Supply-air Temperature Deviating from its Set Point

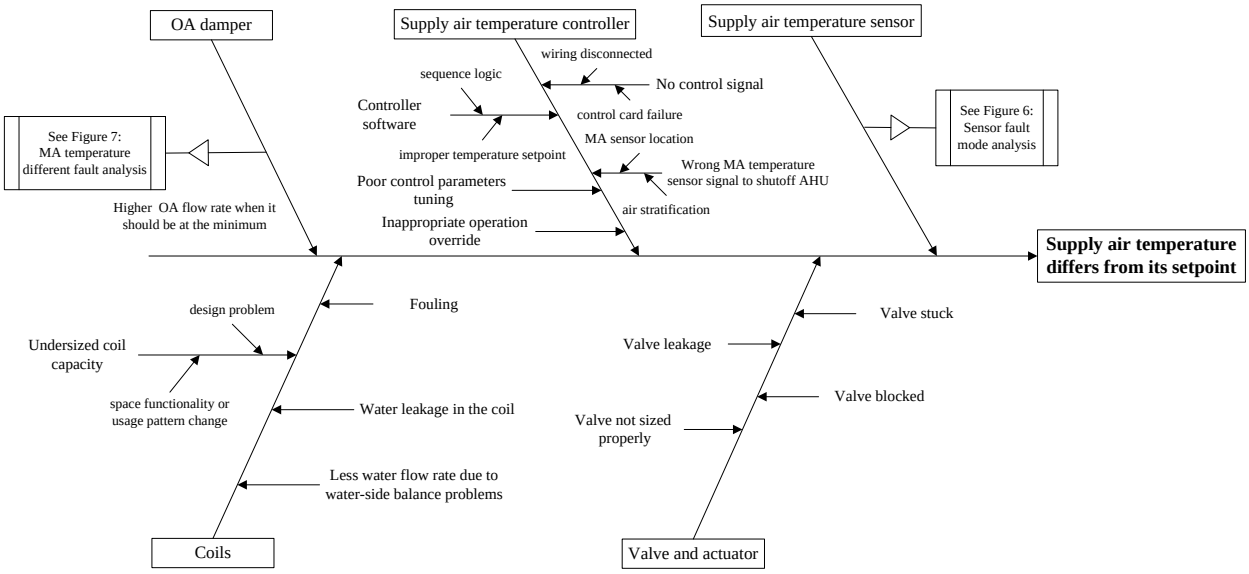

Figure 9: Cause-effect Diagram for the Supply-air Pressure Differing from its Set Point

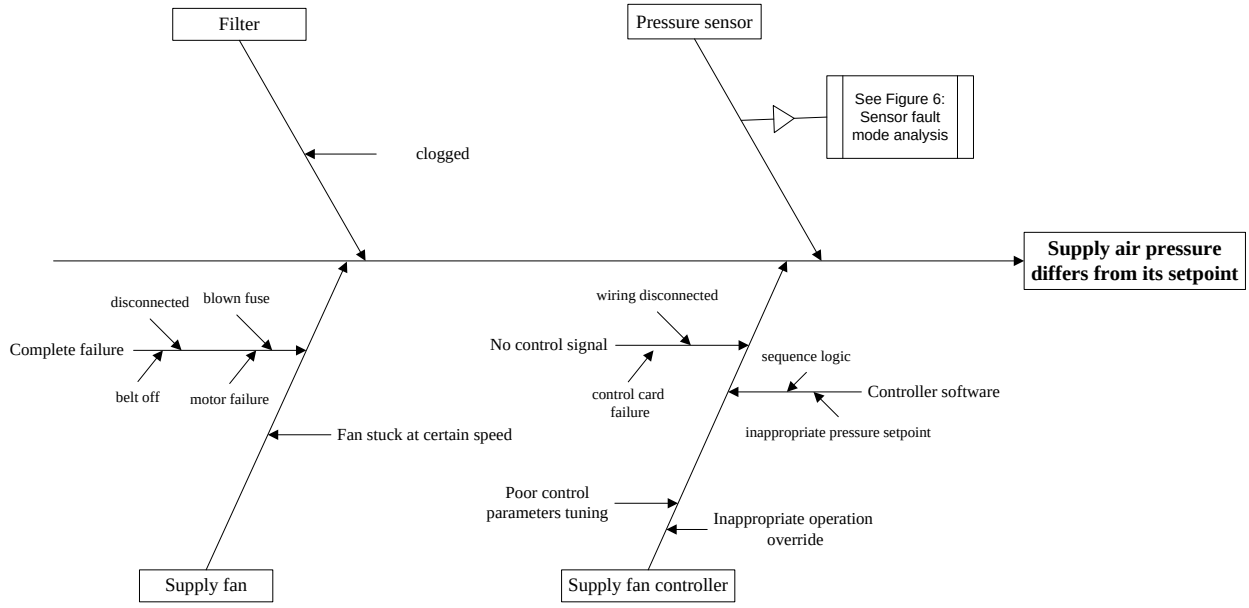

Figure 10: Cause-effect Diagram for the AHU Operation Mode Changing More Frequently than Normal

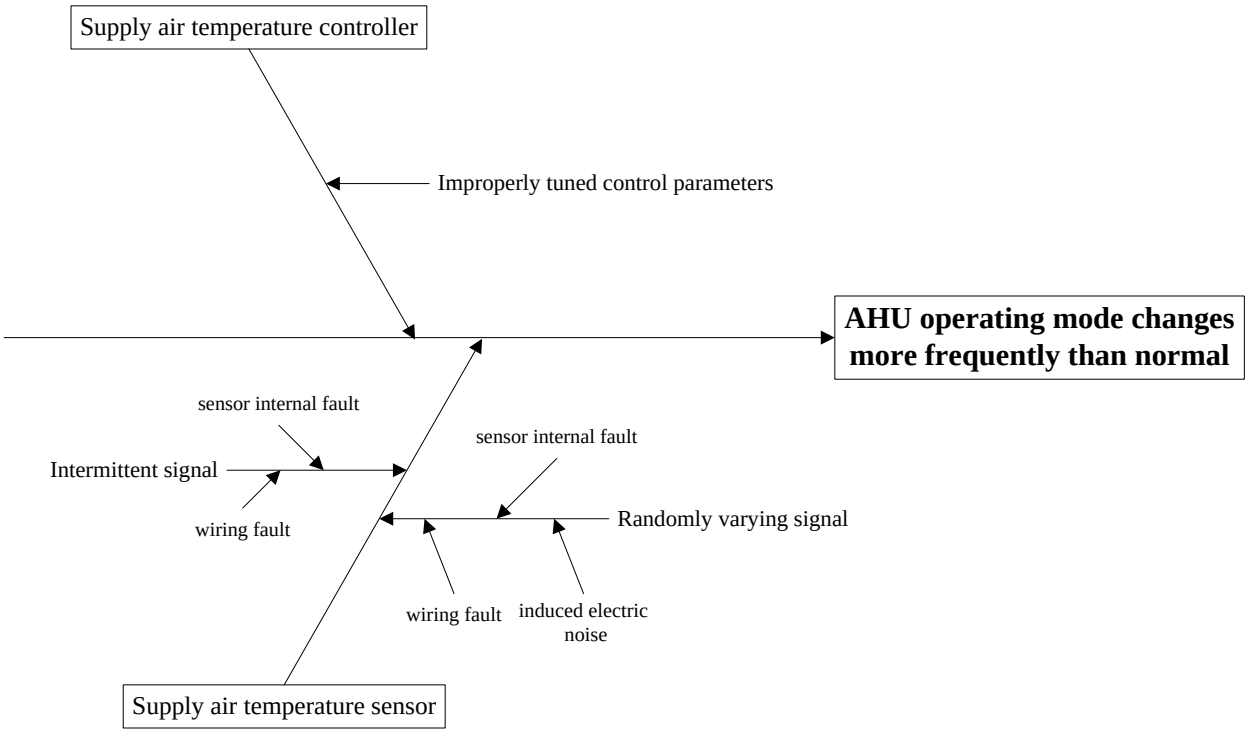

Figure 11: Cause-effect Diagram for the Supply-air Flow Rate Differing from its Value Under Similar Normal Operating Conditions

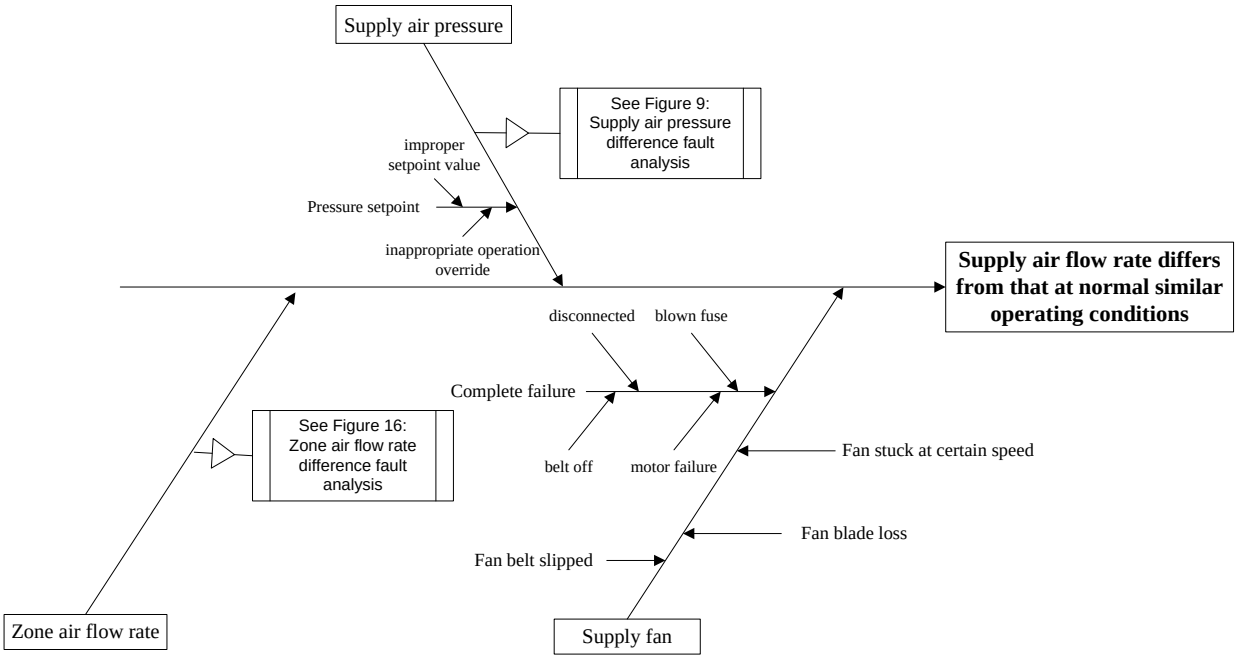

Figure 12: Cause-effect Diagram for the Supply-air Fan Energy Use Differing from Normal Values Under Similar Operating Conditions

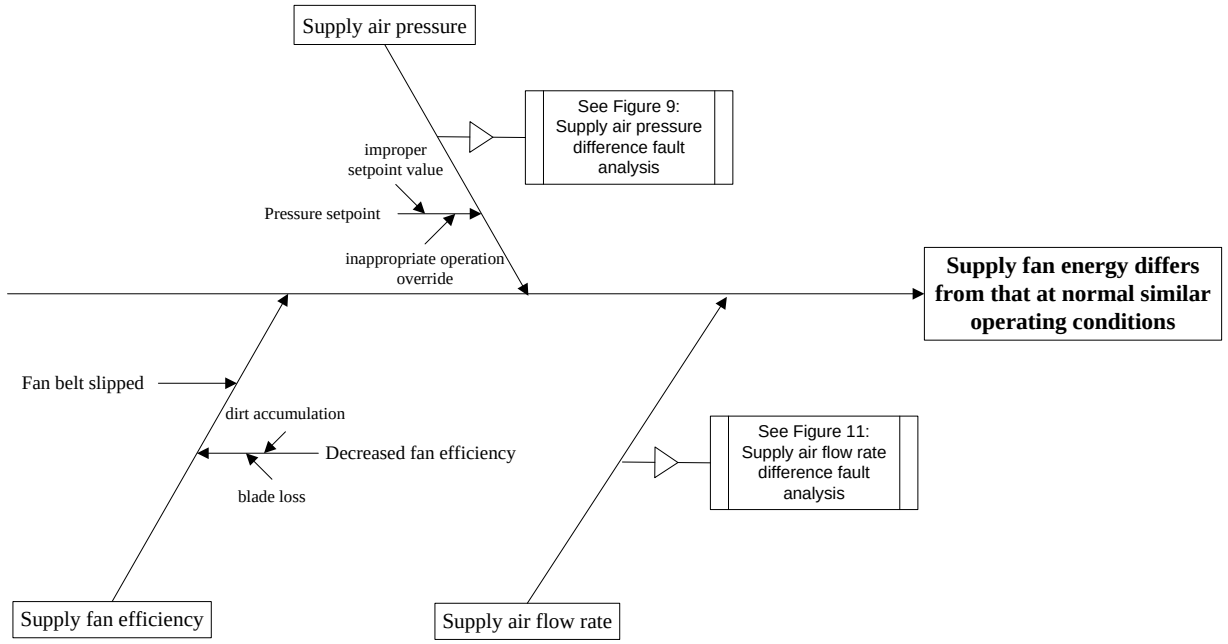

Figure 13: Cause-effect Diagram for the AHU Heating Energy Consumption Differing from Normal Values Under Similar Operating Conditions

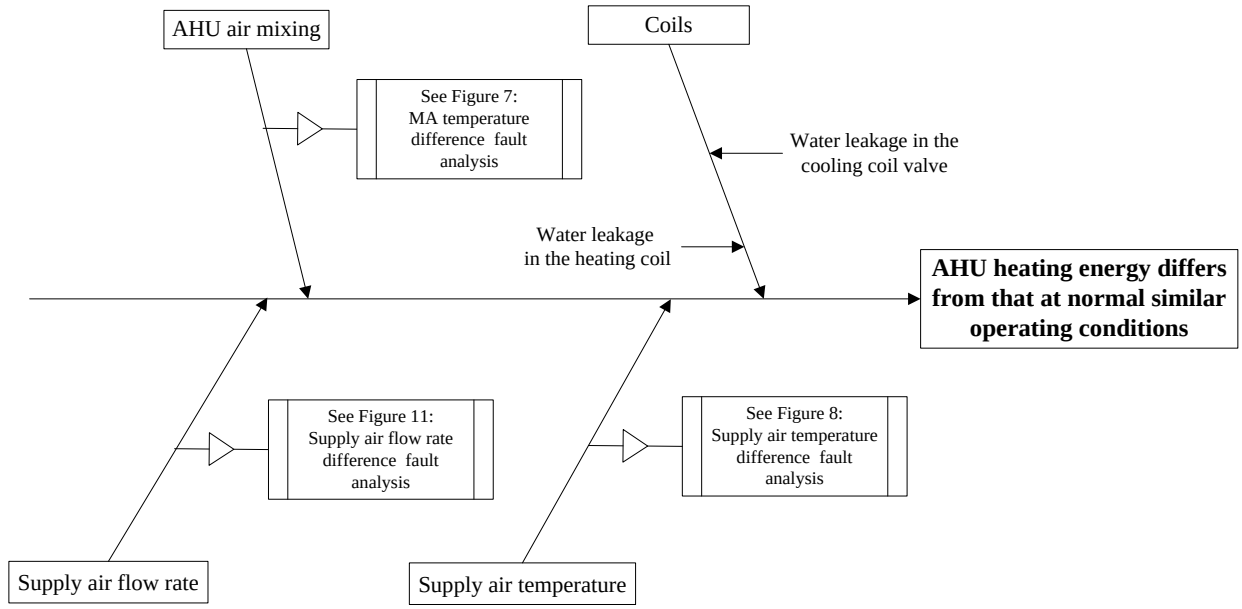

Figure 14: Cause-effect Diagram for the AHU Cooling Energy Use Differing from Normal Values Under Similar Operating Conditions

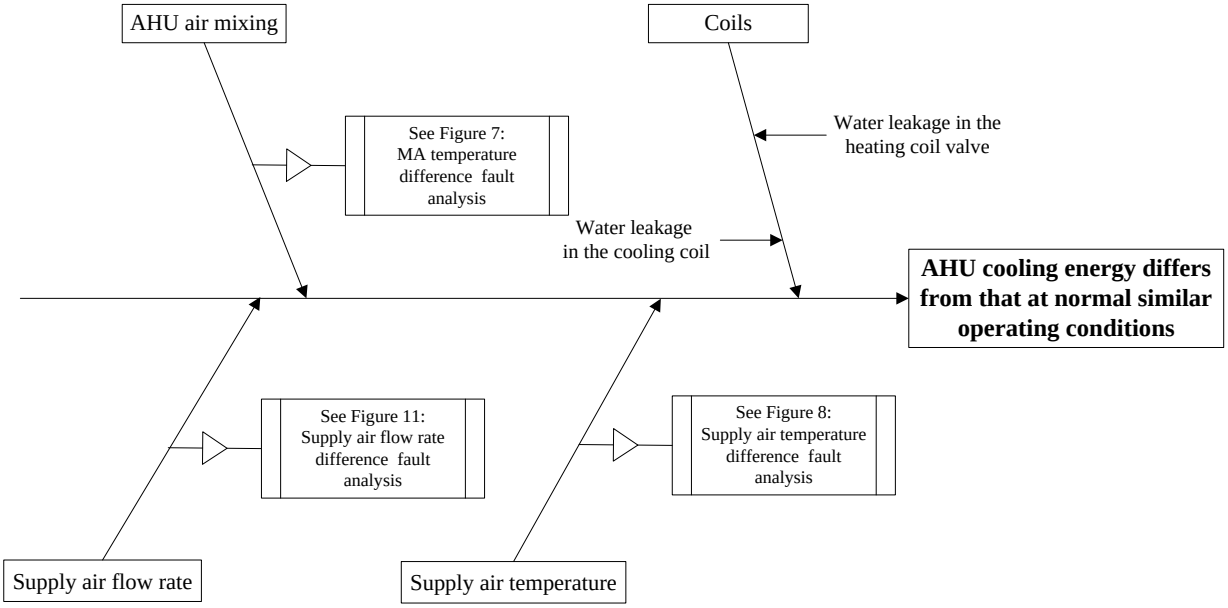

Figure 15: Cause-effect Diagram for Zone-air Temperature Differing from its Set Point

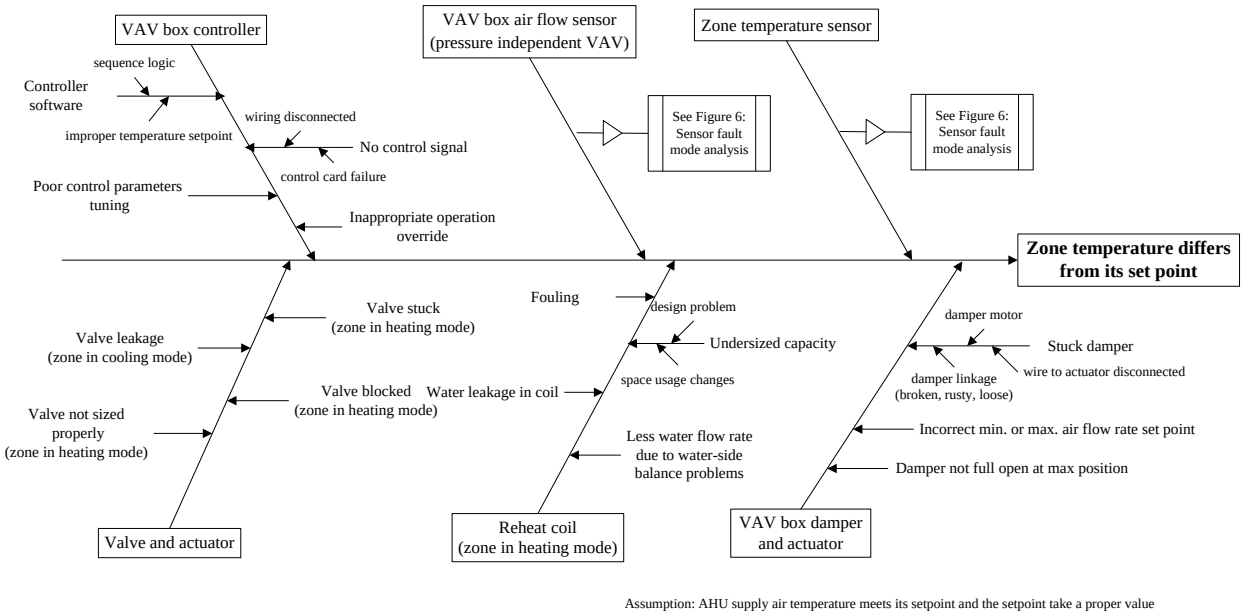

Assumption: AHU supply air temperature meets its setpoint and the setpoint take a proper value

Figure 16: Cause-effect Diagram for the VAV-box Flow Rate Differing from Normal Values Under Similar Operating Conditions

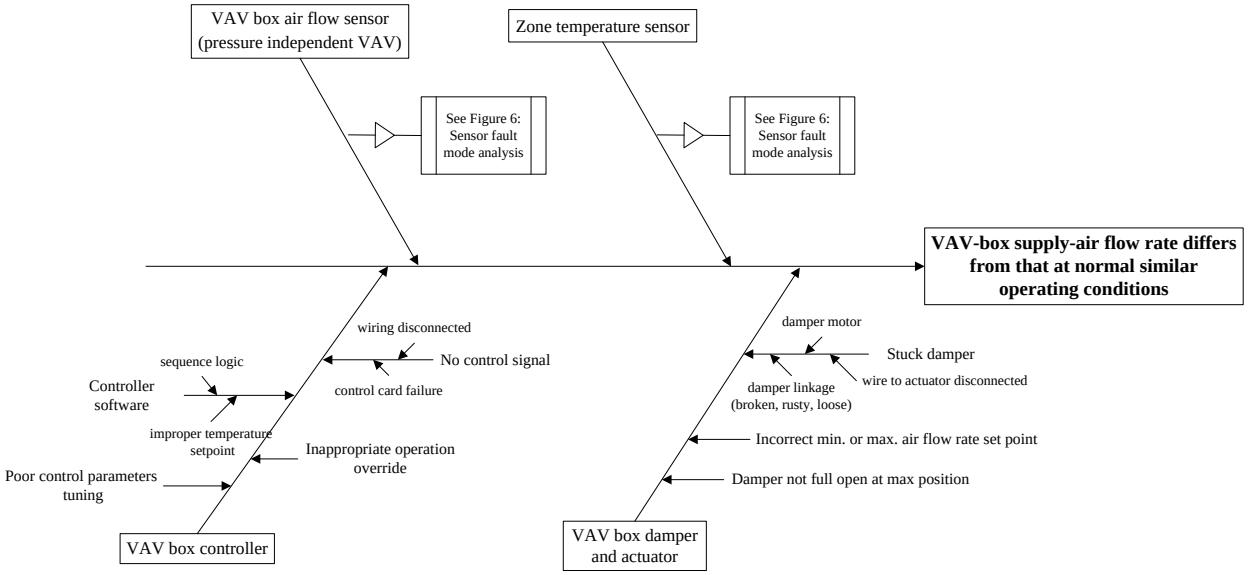

Assumption: AHU supply air temperature meets its setpoint and the setpoint take a proper value

CHAPTER 2:
Algorithm Development

A set of algorithms was developed to facilitate the detection, diagnosis and correction of faults in the air-handling section of VAV systems, based upon the faults identified in Chapter 1 and an understanding of the chain of causation for those faults, developed in the fault mode analysis.

A holistic approach was found important to algorithm development. Analyzing a subsystem in isolation for purposes of fault detection, isolation, and correction is often insufficient. Faults originating outside of a subsystem can manifest as symptoms within the subsystem, and faults originating inside the subsystem can sometimes only be detected as a symptom elsewhere. A holistic approach to SCC, which expands the boundary for analysis beyond the subsystem of interest to all relevant upstream and downstream components, addresses this. For example, the air side of an air-handling system cannot be analyzed independently of the water side of the system. An unexpected temperature measurement on the air side could be caused by a number of factors, one of which is a leaking hot- or cold-water coil.

Another often important consideration is comparison of the measurements by a sensor inside a subsystem with measurements by other sensors outside of that subsystem. For example, to check and correct faulty supply-air flow-rate sensor measurements in an air handler, we use air-flow measurements in the VAV boxes served by the air handler. To be able to use the VAV measurements for this purpose, the model used for fault diagnosis must be extended beyond the air handler (i.e., the subsystem) itself to the VAV boxes it servers. So, while we originally planned to develop algorithms for the air-handler filter, fan, and coil section alone, the analysis performed by the algorithms was extended to include VAV boxes as well.

As another example, consider a supply-air fan that is inducing a lower air flow rate than expected. This could have at its root a problem with the fan itself, such as a slipping belt. The problem could, however, be stuck dampers either upstream or downstream of the filter/fan/coil section (i.e., outside air dampers or VAV dampers) that cause increased air-flow resistance. In development of the algorithms, all components that affect the air side of the VAV system are considered. Fernandez et al. (2009a) developed algorithms for the mixing-box section of an air handler. In this report, algorithms for fault detection, isolation and self-correction in all components downstream of the mixing box are considered. These algorithms are presented in detail in Fernandez et al. 2011, which provides more detailed descriptions of the algorithms than presented here and the full set of flow charts. Table 5 provides a full list of the faults that may lead to detection of a fault within those algorithms. For each fault, Table 5 also specifies whether it can be diagnosed through automatic or proactive diagnostic processes, and whether it can be automatically corrected.

The algorithms are developed in such a way that they can be easily implemented in a software package that interfaces with an actual system in a laboratory for testing. Figure 17 provides an overview of the process developed at the system level. A red, dotted line encloses a box that conceptualizes the control system loop that the VAV system uses. In a system without self-correcting controls, this process is a simple loop that involves taking measurements from sensors, calculating control signals using the sensor readings as inputs, and then controlling the system via the actuators (valves, dampers, etc.) to which the control signals are sent. In the self-

Table 5: Faults Detectable in Algorithms Developed for CIEE Algorithms report

Type of Fault	Fault Diagnosed?	Fault Corrected?
Hunting CC valve	Yes	Yes
HC/CC valve controller software logic fault	Yes	Yes
Fan controller software logic fault	Yes	Yes
Supply-air flow station complete failure	Yes	No
Supply-air fan complete failure	Yes	No
Supply-air fan belt slipping/decreased fan η	Yes	No
Supply-air flow station biased	Yes	Yes
Supply-air flow station erratic	Yes	No
CC valve stuck open or leaking	Yes	No
HC valve stuck open or leaking	Yes	No
MA temperature sensor biased	Yes	Yes
MA temperature sensor erratic/not working	Yes	No
HC temperature sensor biased	Yes	Yes
HC temperature sensor erratic/not working	Yes	No
SA temperature sensor biased	Yes	Yes
SA temperature sensor erratic/not working	Yes	No
Filter is clogged/oversized	Yes	No
Filter differential pressure sensor biased/ erratic/not working	Yes	No
Filter has fallen down or is installed incorrectly	Yes	No
VAV box damper does not modulate in upper half of signal range	Yes	No
VAV box damper does not modulate in lower half of signal range	Yes	No
VAV box flow sensor is biased	Yes	Yes
VAV box reheat coil valve stuck open or leaking	Yes	No
Discharge air temperature sensor biased	Yes	Yes
Discharge air temperature sensor erratic/not working	Yes	No
VAV box flow station erratic/ not working	Yes	No
VAV box damper stuck	Yes	No
VAV box incorrect maximum flow set point	Yes	Yes

Figure 17: Master Flowchart for Self-Correcting Controls

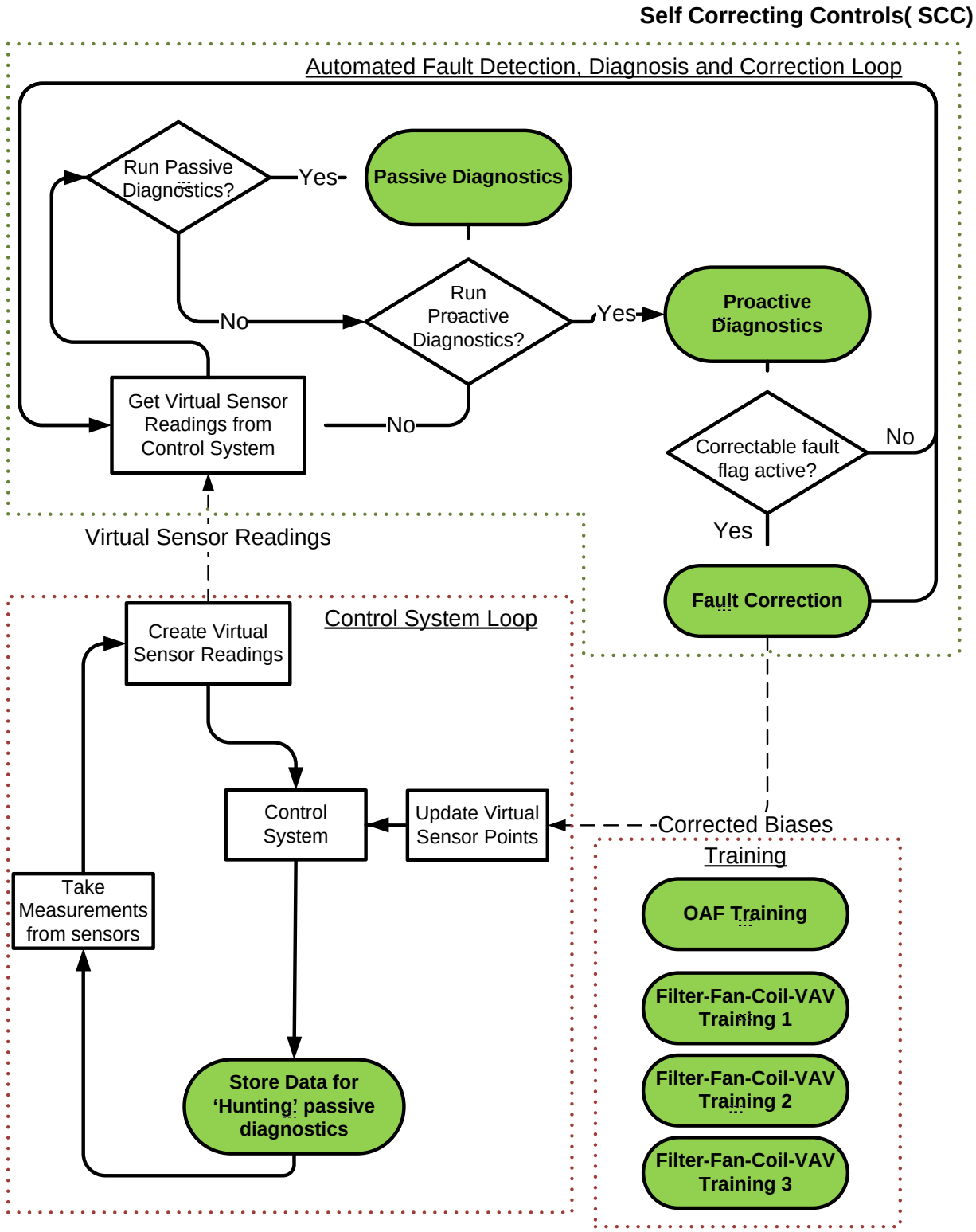

correcting controls process, there are additional steps in the process. The actual sensor measurements are input to virtual sensors, which generate corrected sensor values (when warranted). The corrected virtual values are then used by the control algorithms in place of erroneous sensor readings so that the controller sends the correct actuation signal to the actuator. From the standpoint of control, these virtual sensor readings replace the actual readings.

A green dotted line in Figure 17 encloses a separate process that executes simultaneously with the control system loop. This process is the automated fault detection, diagnostics, and correction loop (AFDDC). This process takes in sensor data from the virtual sensor points as well as control code information from the control system and continuously monitors those values for signs of faults.

As long as no faults are detected, the system runs through a sub-loop within this process that periodically checks for faults. The process of checking for faults is called Passive Diagnostics because faults are detected through passive, observation monitoring only, without affecting the control process.

When a fault is detected by the passive diagnostics, a process called ***Proactive Diagnostics*** is initiated. The proactive process diagnoses (or isolates) the fault. For example, passive diagnostics may detect that a set of sensors is displaying readings that are inconsistent with one another based on the physical relationships among the measured variables. Proactive diagnostics determine which, if any of the sensors, is reading improperly, or if the detected inconsistency might be caused by something like stuck dampers or leaking valves that produce the unexpected (abnormal) measured conditions. Proactive diagnostics involve taking control of the system away from its ordinary automatic operation and placing it into alternative states controlled by the AFDDC software. The AFDDC software places the system into specific conditions that enable isolation of the fault to a specific component (or cause). The proactive diagnostics can run automatically, immediately upon fault detection, can be scheduled to run at specific times, or can be run manually, when it is convenient for the building operator or occupants.

Once the fault has been successfully diagnosed, the AFDDC ***Fault Correction*** process starts, wherein the specific component is recalibrated so that its fault can be automatically accounted for by the control system via the creation of a new virtual sensor point. This is only possible, however, for "soft faults" or faults that exist in automatically correctable sensors or in the control code itself. The criteria for a sensor being automatically correctable varies, but generally involves having a working sensor available somewhere else in the system or a model that can be used along with correct measurements of other conditions in the physical process to infer the correct value that the faulty sensor would provide if it were working properly.

Another dotted line in Figure 17 encloses a set of ***Training*** processes. Many of the fault detection algorithms rely on models of the physical system behavior under normal operation. Because each system is inherently different, these models are empirically in an initial training process that could be part of the system's commissioning. In training, the system's normal (fault-free) operation is empirically and quantitatively characterized.

Training

Four training algorithms are grouped under the set of training processes shown in Figure 17. The first one, titled "OAF Training" is used for detecting mixing-box faults, and is described in Fernandez et al. (2009b). The others are training algorithms for the filter/fan/coil section of the air handler of the VAV system and are described in detail in Fernandez et al. (2009a).

The "Filter/Fan/Coil/VAV Training 1" process, referred to subsequently as Training 1, develops empirical relationships between the normal supply-air flow rate (V_S) and two parameters: 1) U_{SF}, the fan control signal, which is a voltage or current signal sent to the fan and is normalized to a range of 0-100% and 2) U_{damp}, the normalized control signal for the outdoor-air damper. The variable U_{damp} determines the outdoor-air damper position and, as a result, V_S, given a value of the fan speed. While VAV dampers individually can affect air-flow resistance, all the dampers in the VAV boxes served by a specific air handler are typically controlled together to maintain the supply-air static pressure at a fixed value (its set point). This training algorithm fits the collected data to a two-factor polynomial regression equation.

Training 2 develops two empirical relationships. The first relates the normal temperature rise of the air as it passes across the fan (from fan motor heat rejection) as a function of V_S. Measurements of the temperature increase are taken at discrete values of the fan speed over its full range, and are stored as a lookup table. Temperature increases from the fan for values of V_S between the measured values of the table are determined by linearly interpolating. The second relates the normal filter pressure drop to V_S, again based on measurements of the pressure drop across the filter at selected values of V_S over its full range. The measured results are stored in a lookup table and values of pressure drop for intermediate values of V_S are obtained by linear interpolation.

Training 3 develops an empirical relationship between ΔT_{SM}, which is the difference between the supply-air temperature and the mixed-air temperature, and two variables, V_S and the control signal for the chilled-water valve of the cooling coil, U_{CC}. Measurements are made and a polynomial curve fit is used to establish the relationship.

Passive Diagnostics

Figure 18 shows the main passive diagnostics process for the filter/fan/coil and VAV box sections. The passive diagnostics process is serial, executing a set of algorithms sequentially until a fault is found, at which point the Passive Diagnostics process terminates and the proactive diagnostics process begins (according to how it is scheduled) or until all of the algorithms have passed without detection of a fault.

Key information can be obtained from the passive diagnostics about the nature of the fault that dictates which proactive tests are necessary to isolate and diagnose the fault. The specific passive diagnostic rule that detects the symptom of a fault provides one clue. Other clues can sometimes be obtained from the sequence of passive diagnostic tests. For example, if Fault 1 always causes both symptom A and symptom B, and Faults 2 and 3 cause symptom B, but not symptom A, then if the occurrence of symptom A is checked before the presence of symptom B and found not to be present, Fault 1 can be ruled out when symptom B is present. This type of logic is employed in the passive diagnostic algorithms through use of a set of "flags." These

Figure 18: Passive Diagnostics for Filter/Fan/Coil/VAV Boxes

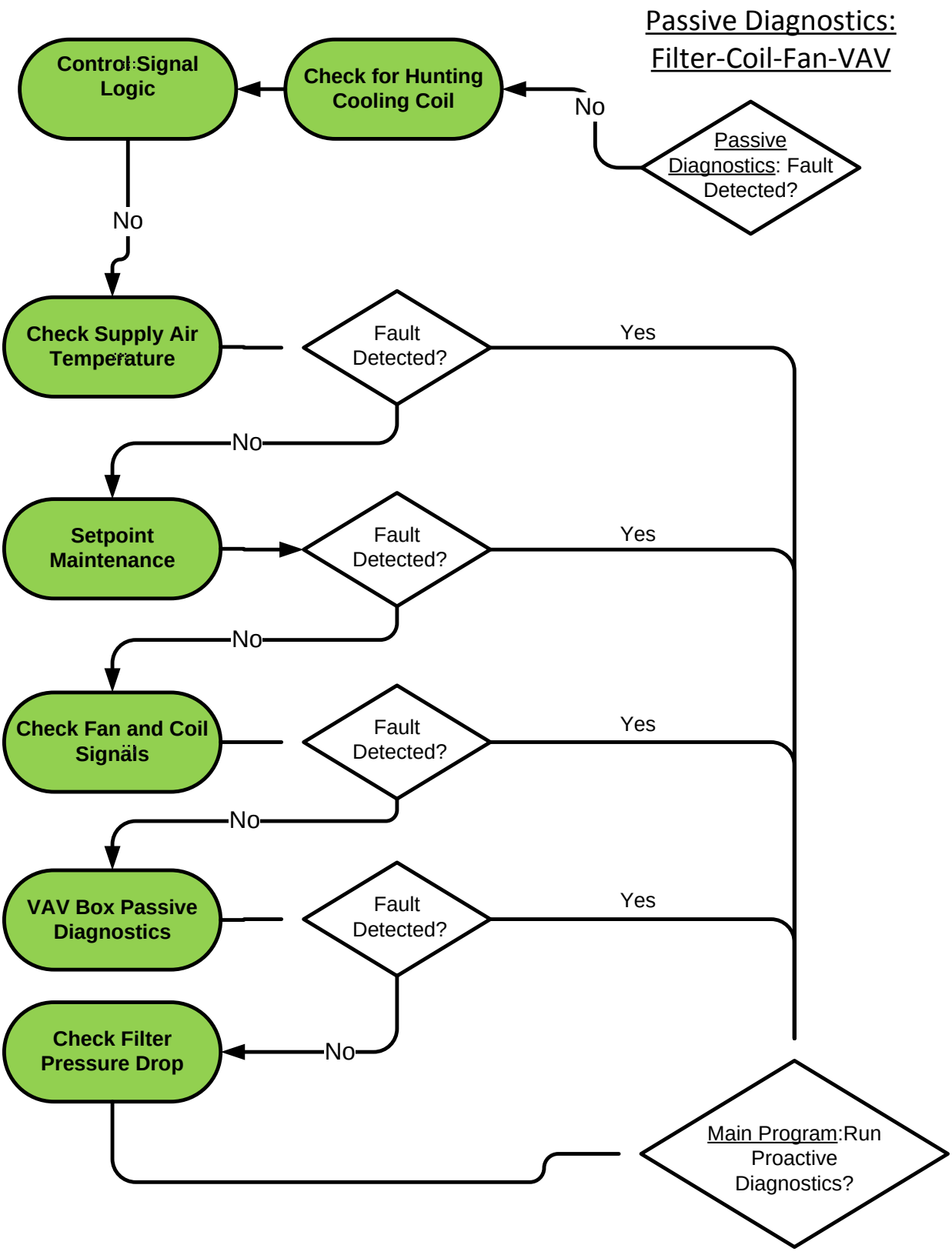

numbered flags are raised at specific points in the passive diagnostic process when faults are detected. The flags then direct the flow of proactive diagnostic tests so that only the remaining tests necessary to diagnose the observed symptom are performed.

Descriptions of the individual algorithms run sequentially in the passive diagnostics follow [see also Fernandez et al. (2011)].

Check for Hunting Cooling Coil – This algorithm checks that the cooling coil valve is not "hunting." A hunting actuator is one that oscillates around the position it is seeking. Poorly set values of control constants in the proportional-integral (PI) or proportional-integral-derivative (PID) controller for the cooling coil valve actuator can cause this. The algorithm for checking for hunting uses a database of past cooling coil command signals to detect whether hunting is taking place. No proactive diagnostics are needed to detect this fault.

Control System Logic – This algorithm checks to ensure that flow through the air-handler heating coil and cooling coil do not occur at the same time. It checks whether both the heating and cooling coils are properly off when the system is economizing with the outdoor-air damper signal $U_{damp} < 100\%$ open and that the heating coil is off when the system is economizing at $U_{damp} = 100\%$. Violation of these faults indicates incorrect control algorithms for the air-handler damper system, and can be automatically corrected with a correct algorithm upon detection; no proactive diagnostics are needed to isolate the fault.

Check Supply-air Temperature – This algorithm uses training data from Training 2 to determine if the observed fan heat gain matches the training closely enough. This is done by monitoring the difference between the supply-air temperature and cooling coil inlet temperature. If the heating and cooling coils are off, the allowable supply-air temperature is bound on both sides by temperature tolerances to the temperatures expected from Training 2. If one of the coils is commanded on, the allowable supply-air temperature is only bounded on one side, i.e., if the cooling coil is on, the algorithm checks to make sure the supply-air temperature sensor is not reading *higher* than the cooling coil inlet temperature plus the fan temperature rise and the temperature tolerances.

Set Point Maintenance - This algorithm checks whether both the supply-air temperature and supply-air static pressure are correctly within acceptable ranges of their set points. If the supply-air temperature cannot maintain its set point, but the coils are not being commanded on, or if the supply-air static pressure cannot maintain its set point, but the fan is not being commanded on, this indicates a control software (or algorithm) fault that is automatically correctable. Otherwise, these conditions might indicate a fault somewhere else in the system.

Check Fan and Coil Signals – This algorithm uses the regression equations from Training 1 and Training 3 to determine if a) the current value of the coil coil control signal, U_{CC}, is providing the expected degree of cooling, as measured by the difference between the supply-air and mixed-air temperatures, given the current supply-air flow rate and b) if the current value of the supply-fan control signal, U_{SF}, is providing the expected supply-air flow rate, given the current outdoor-air damper position. Readings that are outside of acceptable ranges could indicate a number of different faults.

VAV Box – This algorithm checks the sensor measurements from the VAV boxes for symptoms of faults. First, for each VAV box whose reheat coil has been off for at least 10 minutes and whose damper is at least partially open, it checks whether the VAV-box discharge-air

temperature is correctly within specified tolerances of the supply-air temperature set point. Next, it checks whether the room temperature is within the proper range of the heating and cooling set-point temperatures. This condition is acceptable, especially given the time delay between detecting that the room temperature differs from its set point by an unacceptable amount and subsequently returning the room temperature to the set point. If the temperatures are outside acceptable tolerance of the set points, the algorithm also checks whether the VAV-box flow meter indicates a box air-flow rate correctly above its minimum set point, and when heating is required, that the reheat coil for the VAV box is commanded on. If these conditions are violated a fault is present.

Check Filter Pressure Drop- This algorithm uses Training 2 data to determine whether the fan's differential pressure sensor is reading within acceptable ranges. If the pressure drop is too high, a clogged filter that needs to be replaced could be indicated. If it is too low, the filter could be missing, have fallen down out of its frame, or have been improperly installed. Low filter pressure drop could also indicate that the sensor itself is faulty or that a fan fault exists. As with most other instances of fault detection, further proactive diagnostics are needed to isolate the specific fault.

Proactive Diagnostics

Proactive diagnostics begin subsequent (either immediately, or scheduled later) to the detection of a passive fault that cannot be automatically isolated and corrected. Figure 19 shows the overall process of proactive diagnostics for the filter-fan-coil-VAV section. Unlike the passive diagnostics, there is more management of the direction of logical flow through this proactive diagnostics process to efficiently schedule the tests - eliminating unnecessary testing.

Proactive diagnostics always start with *Check Fan.* A fan that is completely stuck or not functioning could potentially lead to all of the undiagnosed faults detected in the passive diagnosis. Thus, verifying that the fan is, in fact, working is critical. This test starts by checking that the measured supply-air flow rate matches its baseline values for full, medium and off fan speeds established during training. If the values do not adequately match, the flow rate is verified to increase as the supply-fan command is increased. A failure to meet this criterion could indicate either a broken/unresponsive fan or a supply-air flow station that is not working. A further check is used to differentiate these two potential causes. The filter differential pressure is checked to verify that it increases as the fan control signal is increased. If it too, does not change appreciably, the fault is associated with a broken supply fan. If the differential pressure does change, it implicates a complete failure of the supply-fan air-flow station.

If, on the other hand, the measured flow rate does increase as the fan control signal is increased, either the fan or the flow station has dropped out of calibration compared to its training baseline, but is still operating. A further test in this case checks for two symptoms that may exist if the problem is a decrease in fan efficiency (i.e., fan producing decreased mechanical output for a given control signal – one cause is a slipping fan belt). If this were the only fault, the deviation from training flow rates would be much greater at a full fan control signal 100% compared to the deviation when the control signal is zero (i.e., off). The filter pressure drop would also be lower for each specific fan control signal than the pressure drop during training,

Figure 19: Proactive Diagnostics for Filter/Fan/Coil and VAV Box Sections: Main Flowchart

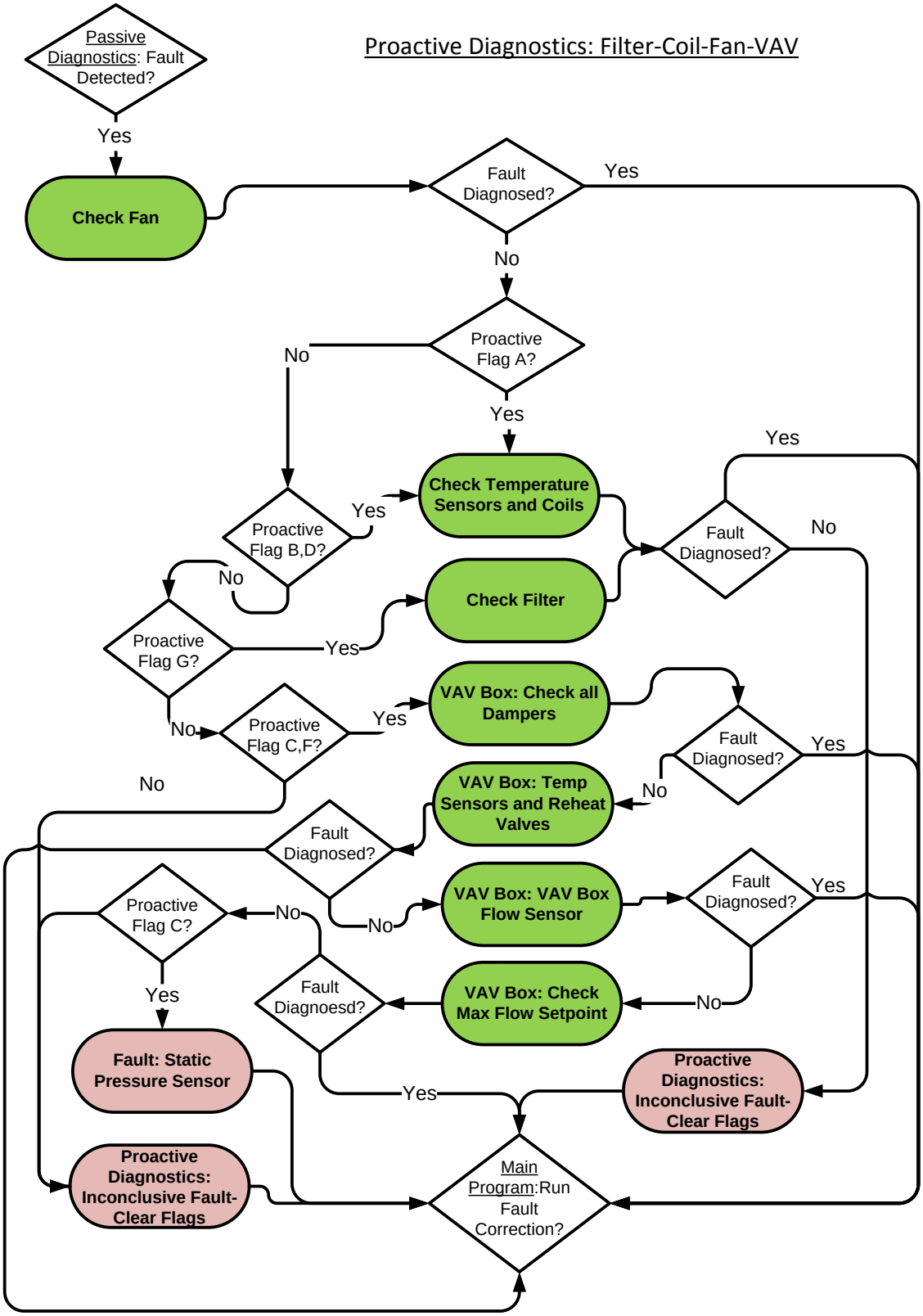

because the fan is not able to drive as much flow and, therefore, not able to establish as strong a pressure drop across the filter. The satisfaction of these two criteria automatically implicates a faulty fan. A partially clogged filter muddies the analysis, however, because clogging may act to increase the filter pressure drop. The assumption here is, however, that a clogged filter alone will not decrease the fan air flow rate sufficiently compared to training baseline values to bypass this entire set of algorithms. If however, the partially clogged filter occurs in conjunction with a slipping fan belt, for instance, it may hinder the detection of the slipping fan belt using this process (flowchart) alone. Thus, a somewhat redundant algorithm is used to distinguish between these different situations. This algorithm compares the measured supply-air flow rate against a few the individual VAV box measured flow rates. This requires closing all of the VAV dampers but one and measuring the flow rate at the fully open damper. Normal leakage through the network of closed dampers and ductwork needs to be accounted for (which is the purpose of the leakage flow testing performed in training). This training-based leakage flow is subtracted from the measured supply- air flow rate before comparison to the VAV box measured flow rate. If the two flow rates roughly match, the result implicates decreased efficiency of the supply fan, whereas if the values do not match adequately, this implicates a working, but faulty, supply-air flow station.

If no faults are found in the fan or flow station, the measured flow rate should be reasonably close to the baseline (training) value, and selected proactive tests can then be scheduled according to clues from the passive diagnostics. If Proactive Flag A,B, or D is active (these flags are raised in response to several conditions in the passive diagnostics; see Fernandez et al. 2011), the *Check Temperature Sensors and Coils* process is performed. A fault can be traced to one of the three air-handler temperature sensors (mixed air, cooling-coil inlet air, or supply air) or to a leaking heating or cooling coil. Fault isolation is accomplished by setting the heating and cooling coil control signals to zero and monitoring the differences between the values of the three mixing-box temperature sensors at three fan speeds: low, medium, and full. Much of the differentiation relies on the temperature difference across a leaking heating or cooling coil decreasing with increased air-flow rate (even as the total heating or cooling imparted to the air stream increases). If the temperature change across the coils does not decrease with increasing flow rate, the fault is almost certainly with one of the temperature sensors, which can then be isolated by checking the three sensor readings against each other, accounting for fan temperature rise.

The *Check Filter* process follows next. It runs when a flag for a fault occurs in the filter check during the passive diagnostics (and no faults have been isolated thus far). *T*he algorithm isolates physical filter faults from pressure-drop sensor faults by setting the supply fan to zero and checking the measured pressure drop. If it is non-zero, the fault is isolated to the pressure sensor. If the pressure drop reads zero with the fan off, the fault is isolated to either a clogged filter, if the pressure drop was higher than the training value when the fault was detected, or to a missing, fallen or improperly installed filter, if the pressure drop was lower than the training value when the fault was detected.

After the *Check Filter* process is completed, all potential faults in the air-handler filter-fan-coil section have been considered, leaving faults in the VAV boxes undiagnosed. When a flag is raised in the passive diagnosis that indicates the possibility of a VAV-box fault, four VAV box tests is performed sequentially until a fault is isolated.

The first test for VAV boxes, *VAV Box: Check All Dampers*, uses sensed data for a range of fan speeds for all VAV boxes to isolate either faulty dampers or faulty VAV-box flow sensors in any of the VAV boxes. Stuck dampers and completely non-functional VAV-box flow stations are indistinguishable at this point. If one of these faults exists, a new flag is raised, and an additional test is used to isolate the fault.

If no faults are found in the VAV-box flow stations and there is a flag for a specific faulty VAV box from the passive diagnostics, the next algorithm, *VAV Temperature Sensors and Reheat Valves* runs. This process differentiates between faulty (leaking or stuck) VAV-box reheat valves and faulty VAV discharge-temperature sensors by checking for a coil heat-gain signature (decreasing temperature difference across the reheat coil at increasing air-flow rate). If this signature is present, the fault is traced to a leaking or stuck open reheat valve. If instead the temperature difference across the reheat coil (difference between the VAV-box discharge air temperature and the temperature of air entering the VAV box) is unchanged or increases , the fault is traced to the discharge-air temperature sensor itself. If the discharge-air temperature remains constant at all reheat coil command signals, the fault is traced to a reheat coil valve that is stuck closed. Otherwise, no faults related to VAV box temperature sensors or coils can be diagnosed.

If no faults have yet been diagnosed in the VAV box, the *VAV Box Flow Sensor* process is used to isolate a faulty VAV-box flow-rate sensor. In this process, the VAV-box flow rate is checked against the supply-air flow rate at low fan speeds, when all other VAV-box dampers are completely closed. The assumption here is that at low fan speeds there will be negligible leakage flow through the other dampers. This assumption needs to be verified. If it is not a valid assumption, further data collection (training) may be required to quantify low-fan speed VAV system leakage (in addition to the full-speed leakage already performed). If the VAV-box flow rate does not match the supply-air flow rate, the result indicates a faulty VAV flow meter. If the readings match and Flag H is active, the fault is traced to a stuck VAV-box damper.

If no faults are detected after completion of the *VAV Temperature Sensors and Reheat Valves* process, one final VAV diagnostic test called *VAV Box Maximum Flow Rate Set Point* is performed. This process tests whether the VAV box can meet its maximum flow-rate set point. At this point, all other components of the VAV box have been verified to be working properly, so this test should represent a conclusive test of the VAV box's capability. If it passes this test, the detection of a fault in the passive diagnostics may have been an aberration, and the diagnostics should be reset, the system returned to normal operation, and the passive diagnostics instigated once more. There is one exception to this, however. If the supply-air pressure sensor could not meet its set point (leading to Proactive Flag C), and all other components and processes are determined function properly within the proactive diagnostics, the supply-air pressure sensor is deemed to be faulty by the process of elimination. There is no other way to test this sensor for a VAV system as instrumented.

Fault Correction

Figure 20 shows the overall process flowchart for automatic fault correction. Automatic correction of diagnosed soft faults occurs subsequent to their diagnosis in the fault correction process. Two classes of soft faults (software errors and hunting) are corrected automatically as

Figure 20: Fault Correction: Filter/Fan/Coil and VAV sections

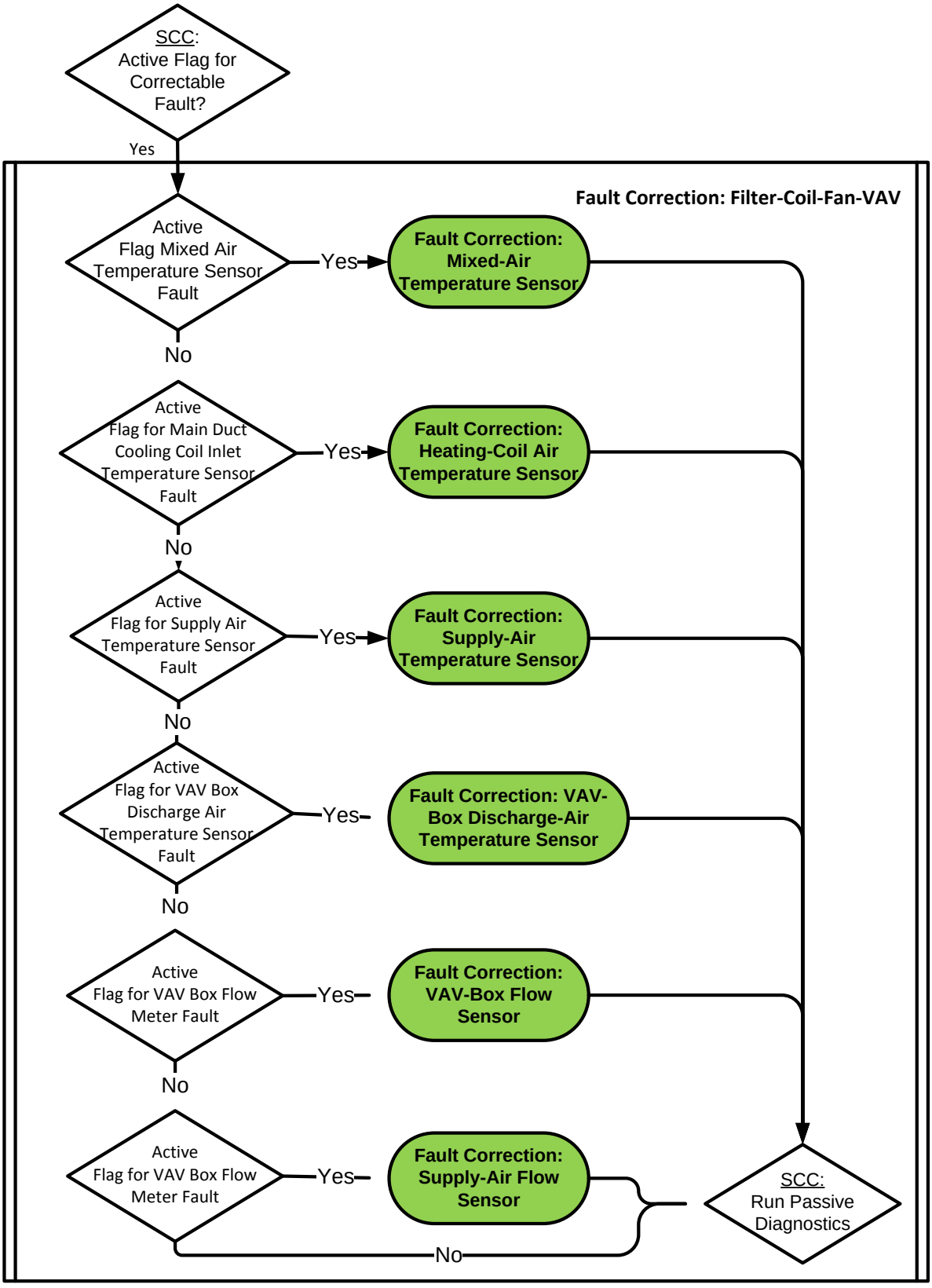

they are detected in the passive diagnostics. This leaves one class of soft faults (sensor biases) that need to be corrected after the proactive diagnostics. There are four types of sensors and two types of flow-rate sensors that can be corrected using the processes presented here. The correction process involves calibrating the faulty sensor against a working sensor in the same airstream. First, however, the behavior of the faulty sensor is checked to determine whether its output is nearly constant over time compared to the working sensor against which it will be calibrated. If the difference is constant, this indicates a bias that can be readily determined and corrected by subtracting a constant value for the incorrect measured value in a virtual sensor placed in the control system loop. If it is not constant, correction of the fault will require a more complex behavioral characterization not developed yet, or the sensor may behave erratically or have failed in some way, both of which require that the faulty sensor be replaced.

The mixed-air and cooling coil inlet air-temperature sensor outputs can be recalibrated directly from the other, unbiased sensor. Likewise the supply-air and any VAV-box air-temperature sensor can be recalibrated directly by using the other. The supply-air flow-rate sensor and any of the individual VAV-box air-flow sensors can be recalibrated to the other, unbiased sensor, but account must be made for air-flow leakage between the measurement points (i.e., using a, albeit simple, model). Most properly working dampers still leak slightly when they are completely closed, so it may not be possible to entirely isolate the flow into any one damper. Therefore, a leakage flow is characterized during Training 2 that can be used in this fault correction. The leakage flow rate is the difference between the supply-air flow rate and the flow rate at any one VAV damper that is open while the rest are closed.

CHAPTER 3:
Implementation and Testing

The algorithms developed to detect, diagnose, and correct faults in VAV systems were implemented for laboratory testing by coding them into a programming package that interacts with Factory Plant Management Interface (FPMI) software. In this project, FPMI is used as a human/machine interface (HMI). FPMI is a web-deployed front-end to the Object Linking and Embedding for Process Control (OPC) server and Structured Query Language (SQL) Database. Using the FPMI client interface, users can monitor live data, specify the control variables and sensor paths, and instigate diagnostic and correction tests, including the instigation of faults. Using a database server, the test data and control variables can be stored automatically. In this way, the algorithms we develop are implemented in software code that is used to control the physical system that has been constructed as a test facility for investigating the performance of the algorithms for automated fault detection and correction.

Description of the Test Facility

Section 3 of Fernandez et al. (2009b) provides a description of the laboratory facility used to test the VAV system algorithms. In brief, the system is composed of a chilled water loop that provides chilled water to the coiling coil of an air handler. The air handler draws outdoor air from the environment and mixes it with return air from the room the air handler is located in. An electric heater maintains this room at a temperature set point. The mixed air flows through the chilled water coil, then through a fan and a flow-rate sensor. The test facility has been updated for this project to include four pressure-independent VAV boxes. From the discharge of air handler, where the flow rate sensor is located, the air stream branches to each of the VAV boxes. Each VAV box includes a damper, discharge-air temperature sensor, and a flow meter.

Implementation of Algorithms

Priorities were set for implementation of the algorithms in software code to ensure compatibility with the available project budget. The goals of this prioritization were the following:

- Code a set of algorithms that enabled testing the entire process (fault detection, diagnostics, and correction), albeit for a limited number of faults
- Focus on automatically-correctable, or soft faults, as opposed to hard faults
- Include faults that had many diagnostic pathways so that diagnosis of the correct fault could be verified
- Include all of the training algorithms, because data from these training tests is a valuable tool for future refinement of the algorithms.

With these goals in mind, a set of algorithms was selected that enabled implementation of faults in the supply-air temperature sensor and the supply-air flow meter, while differentiating these faults from those originating from the cooling-coil valve, the fan, other temperature sensors, and the VAV-box flow sensors.

The algorithms developed and the subset implemented in software are identified in Table 6.

Table 6: Algorithms Developed and Implemented (Coded) for Testing

Algorithms Developed	Algorithms Coded
Training Algorithms	
Filter-fan-coil-VAV section, training algorithm 1: expected fan signal	✓
Filter-fan-coil section of VAV air-handler, training algorithm 2: single-factor variables	✓
Filter-fan-coil-VAV section, training algorithm 3: expected cooling coil valve signal	✓
Passive Diagnostics Algorithm for Control System Loop	
Control system loop: store data for hunting passive diagnostics	
Passive Diagnostics Algorithms	
Automatic detection and correction of hunting	
Control system logic	
Check supply-air temperature	✓
Set-point maintenance	
Check fan and coil signals	✓
Check filter pressure drop	
Proactive Diagnostics Algorithms	
Check fan	✓
Check supply-air flow sensor	✓
Temperature sensors and coil valves	✓
Check filter	
VAV: Check all dampers	
VAV: Temperature sensors and reheat valves	
VAV: VAV-box flow sensors	
VAV: VAV-box maximum flow rate set point	
Fault Correction Algorithms	
Mixed-air temperature sensor	
Cooling-coil inlet-air temperature sensor	
Supply-air temperature sensor	✓
Supply-air flow-rate sensor	✓
Control system logic 1	
Control system logic 2	
VAV discharge-air temperature sensor	
VAV flow sensor	

Results

Analysis of Training Data

Data from the training provides insight into how parts of the system perform, which can be critical to inform the process of fault detection. The set of algorithms developed here captures the variations of supply-air flow rate with supply-fan command signal and outdoor-air damper position, the temperature rise across the supply fan (from rejected motor heat) and the filter pressure drop with supply-air flow rate, and the temperature change from the mixed air to the supply air as a function of supply-air flow rate and the cooling-coil command signal. The training tests each involved tracking how these key variables change as a function of one or multiple system parameters. Given these "baseline" relationships, faults can be detected when values of these dependent variables differ the values indicated by the baseline (training) values for the same combination of conditions (values of independent variables). This section reports on how the functional variations observed and the empirical relationships captured from laboratory tests. Chapter 5: Future Work describes some proposed changes to the models to better model the relationships among these variables.

Training 1 Algorithm

Training test #1 uses an algorithm designed to capture the supply-air flow rate as a function of the supply-fan command signal and outdoor-air damper position. The supply-fan command signal directly affects the flow rate, while it was postulated that the outdoor-air damper would also affect the flow rate by changing the upstream resistance to air-flow. Figure 21 shows the results of testing. It reveals two things: 1) the supply-fan command signals do not correspond directly to fan speed (e.g., measured in revolutions per minute—rpm) and 2) a weak relationship exists between the outdoor-air dampers position and fan speed for the system tested. The supply fan does not start operating until the command signal rises above 25% or so. Because the relationship between supply-fan flow rate and the control signal, U_{SF}, was modeled by a 2nd order polynomial, the regression process does not fit the constant supply-fan flow rate of zero for values of U_{SF} less than 25% well. The model gives values less than zero for values of the fan control signal less than 25%. The fit of the model for U_{SF}<25% could be improved by creating a two-region model with the first region for U_{SF}<25% giving a constant value of zero and the second region for 25%<U_{SF}≤100%. In the second region, the flow rate would be represented by a second-order polynomial fit to measured data. The second observation from the training is that, at least for the laboratory test system, there is only a weak relationship between the outdoor-air damper position and fan speed, with the fan speed peaking at intermediate damper positions (compared the relative positions of the different shades of data points and curves in Figure 21). This relationship will likely change from system to system, however, at this point in the development process, the polynomial model is retained, but this may be reconsidered in future work.

Training 2 Algorithm

Training 2 includes models of two relationships, the temperature rise across the supply fan (from rejected motor heat) and the filter pressure drop, each as a function of supply-air flow rate.

In the process of developing the algorithms, it was postulated that the heat gain across the supply fan would decrease with increasing flow rate because higher air-flow rate would dissipate the heat released over a greater mass of air, but this neglected the higher motor power

(and heat dissapated) with higher fan speeds. The temperature diffeence increases at low fan speeds, reaches a local minimum at around 230 CFM, and then increases steadily through the highest flow rate measured, as shown in Figure 22.

Figure 21: Training 1 Data: Expected Supply-Air Flow Rate. Data points and polynomial line fits to the data for different values of the outdoor-air damper signal (U_{damp}) are distinguished by different shades.

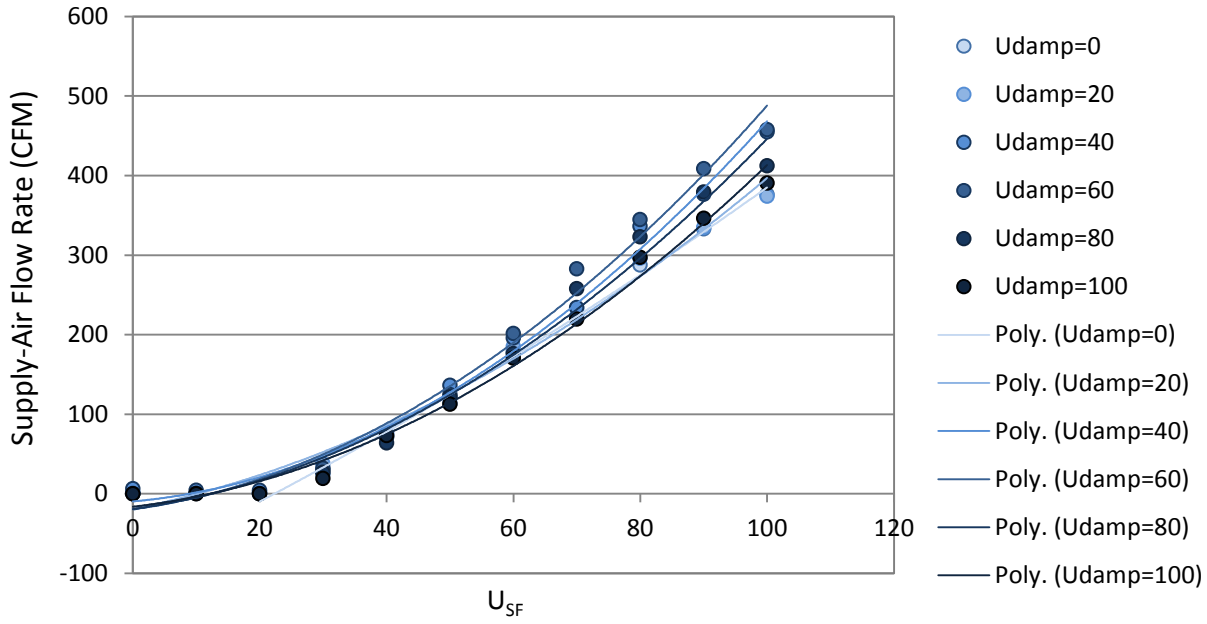

Figure 22: Temperature Rise Across the Supply-Fan as a Function of Supply-Air Flow Rate

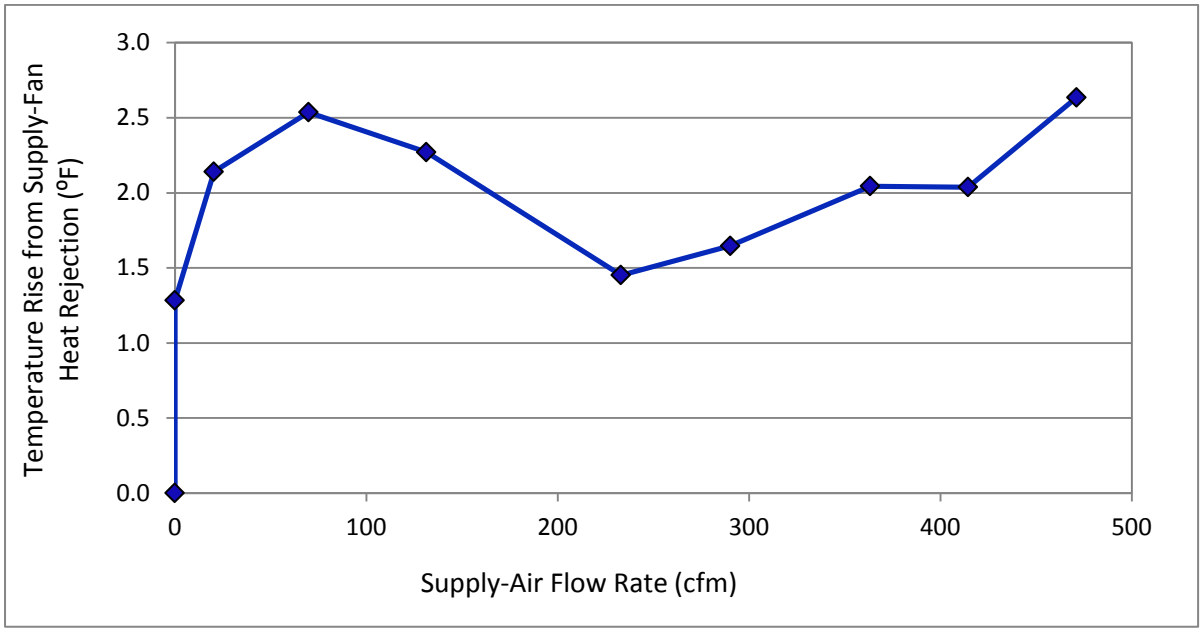

The filter pressure drop exhibited the expected relationship of increasing pressure drop with supply-air flow rate, as shown in Figure 23.

Training 3 Algorithm

A 2nd order polynomial regression was used to fit a model to the measured values of the temperature change from the mixed air to the supply air as a function of supply-air flow rate and the cooling-coil command signal, U_{CC}. Here, there were two issues. First, all control valve signals less than 25% resulted in were equivalent to 0 (i.e., no control action). The second and more important issue is that the test implicitly assumes that there is a constant difference between the mixed-air temperature and the chilled-water temperature. That was not the case in this test, mostly because of poor control over the supply-air temperature. During the test plotted in Figure 24, the chilled-water temperature rose from 52 to 62°F. Hence, the largest temperature drop in the airstream occurred in an intermediate cooling-coil command signal, then dropped as the chilled-water temperature continued to drift higher. Changes in the mixed-air and chilled-water temperatures are very important to account for, and an alternative model for Training 3 is proposed in Chapter 5 that should fix this problem in future work. In any event, chilled-water valve and cooling-coil faults were not investigated in the tests for this project, so the training process can be modified before tests are performed in the future for the algorithms for fault detection, diagnosis and correction processes for those faults.

Figure 23: Measured Filter Pressure Drop versus Supply Air Flow Rate

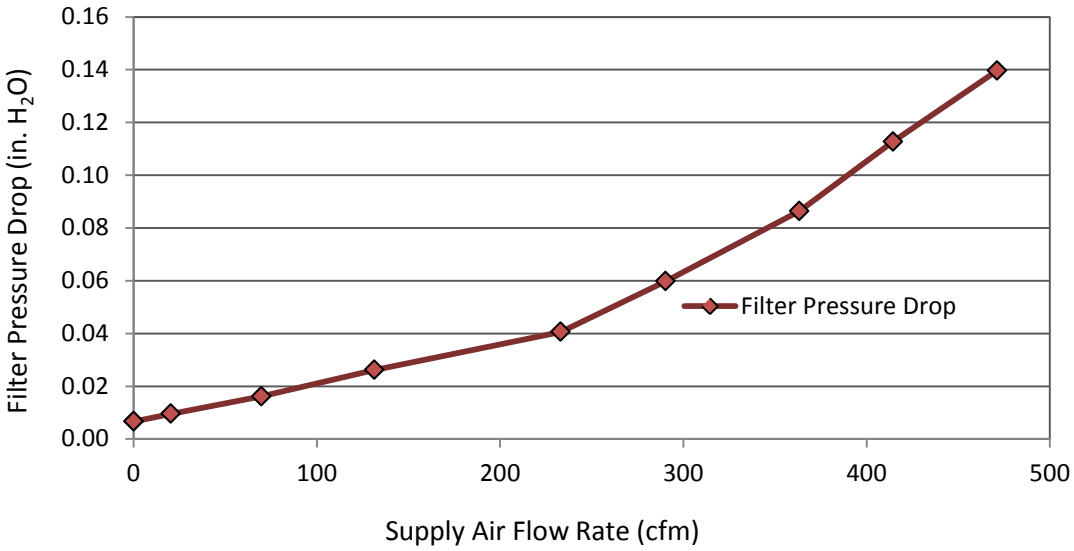

Test Results

Table 7 summarizes the tests of the fault detection, fault diagnostics (isolation) and fault correction processes performed and for which the test results are presented in this section.

Figure 24: Difference Between the Mixed-air and Supply-air Temperatures Plotted against Supply-Air Flow Rate for Values of the Cooling-Coil Control Signal (U_{CC}) from 0 and 100%.

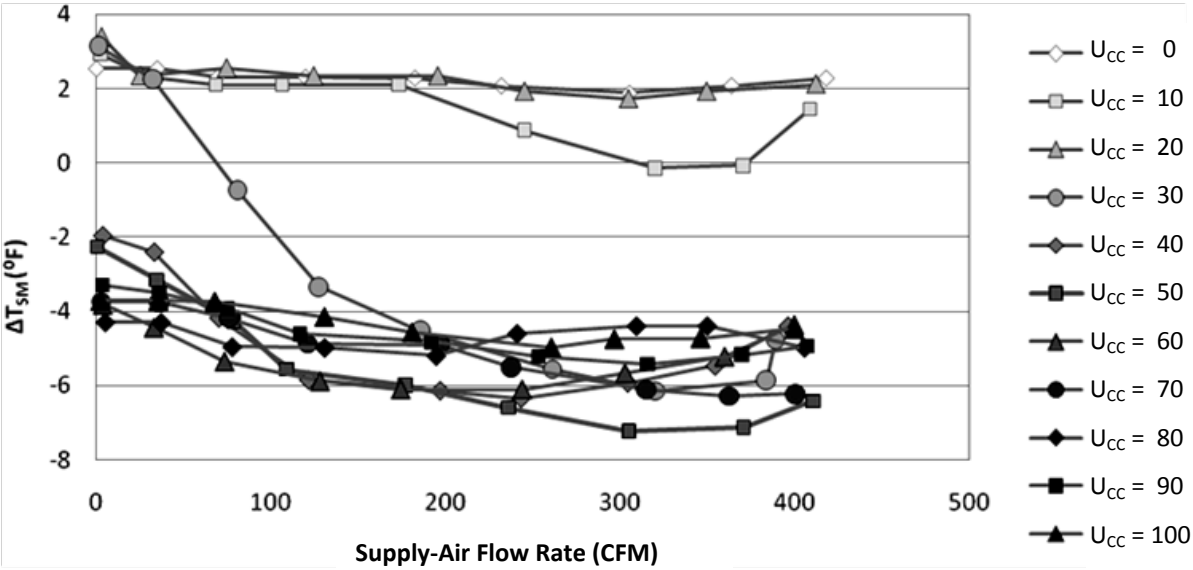

Table 7: Summary of Tests Performed and Primary results. Check marks identify tests that were performed with successful results.

Test Number and Fault Description	Fault Severity	Key Tolerances*	Passive Diagnostics	Proactive Diagnostics	Fault Correction
1. Supply-air Temperature Sensor Bias	+5°F	T_{tol}=2°F $U_{SF,tol}$=10	✓	Inconclusive	
2. Supply-air Temperature Sensor Bias	+5°F	T_{tol}=1°F $U_{SF,tol}$=10	✓	✓	✓ Corrected Bias of +4.1°F
3. Supply-air Temperature Sensor Bias	+8°F	T_{tol}=2°F $U_{SF,tol}$=10	✓	✓	✓ Corrected Bias of +6.6°F

4. Supply-air Flow Rate Bias	+265 cfm (20% of max flow)	T_{tol}=2ºF $U_{SF,tol}$ =10	✓	✓	Concluded that the bias was erratic: replace sensor
5. Supply-air Flow Rate Bias	+265 cfm (20% of max flow)	T_{tol}=2ºF $U_{SF,tol}$ =10	✓	✓	✓ Corrected bias of 287.5 cfm
6. Supply-air Flow Rate Bias	+132 cfm (10% of max flow)	T_{tol}=2ºF $U_{SF,tol}$ =10	✓	✗ Conclusion: Fan belt slipping or decrease in fan efficiency	

*The subscript "tol" designates that the value given represents the tolerance for the variable that it subscripts.

In Test #1, a 5ºF supply-air temperature sensor bias was instigated with a 2ºF temperature sensor tolerances used in the algorithms. The supply-air temperature sensor biases are usually detected with the "Check supply-air temperature" algorithm. The fault is detected as a consequence of the heat gain across the fan exceeding the acceptable range of fan heat gain (at the current supply-air flow rate) during Training 2. The acceptable range is defined according to the tolerances of the temperature sensors. In this case, the test was performed with the algorithms using ±2ºF tolerances applied to all temperature sensors (i.e, assuming that each temperature sensor has an uncertainty of ±2ºF). Because the air temperture increase caused by heat gain from the fan is calculated as the difference between the air temperture downstream of the fan and the the cooling coil inlet temperature (when the cooling coil is off; see Figure 1), the deviation in the temperature difference must exceed the expected training value by 4ºF or more to conclude that the fault exists.

Figure 25 shows the time series of the deviations of the air temperature rise caused by fan heat rejection from its expected value based on the relationship found in Training 1. During the first several minutes of the test, there was no fault implemented, and the fan temperature rise was about 1ºC lower than the equivalent training value. This period is labeled on the figure as point 1. At point 2, a fault is implemented by adding a 5ºF bias to the supply-air temperature sensor output. This brings the air-temperature rise to just over 4ºF, which is the threshold for detection of this fault. The fault is quickly detected at point 3, and proactive diagnostics are started (beginning of region in elipse labeled 4). During the proactive diagnostics, a series of tests is performed (see Fernandez et al. 2011) to isolate the fault as a supply-air temperature sensor fault (rather than being a bias in the mixed-air temperature sensor or a leaking heating coil, among other faults). A problem occurs during the fault isolation process. During the proactive diagnostic testing, at the specific point in the test where the supply-air temperature was

evaluated for bias (point 4a), the fan temperature rise dipped just below the critical 4°F threshold, and the algorithm could not verify that the supply-air temperature sensor was at fault. However, because everything else was working properly, the test could not find a fault anywhere, and the result was a finding of "inconclusive." This was caused by the fault severity being equal to the threshold for fault detection (given the tolerances applied), rather than being a failure of the formulation of the algorithms. When the algorithm decides that there is inconclusive evidence to diagnose (i.e., isolate) a specific fault, it clears all flags that have been raised to run specific diagnostic tests, returns to the passive diagnostics, and begins looking for faults again. If the bias is persistent, it should be detected again, and perhaps if the conditions are right the next time, it would be diagnosed correctly.

Figure 25: Test 1 - Deviation of Fan Temperature Rise From Baseline Training Value

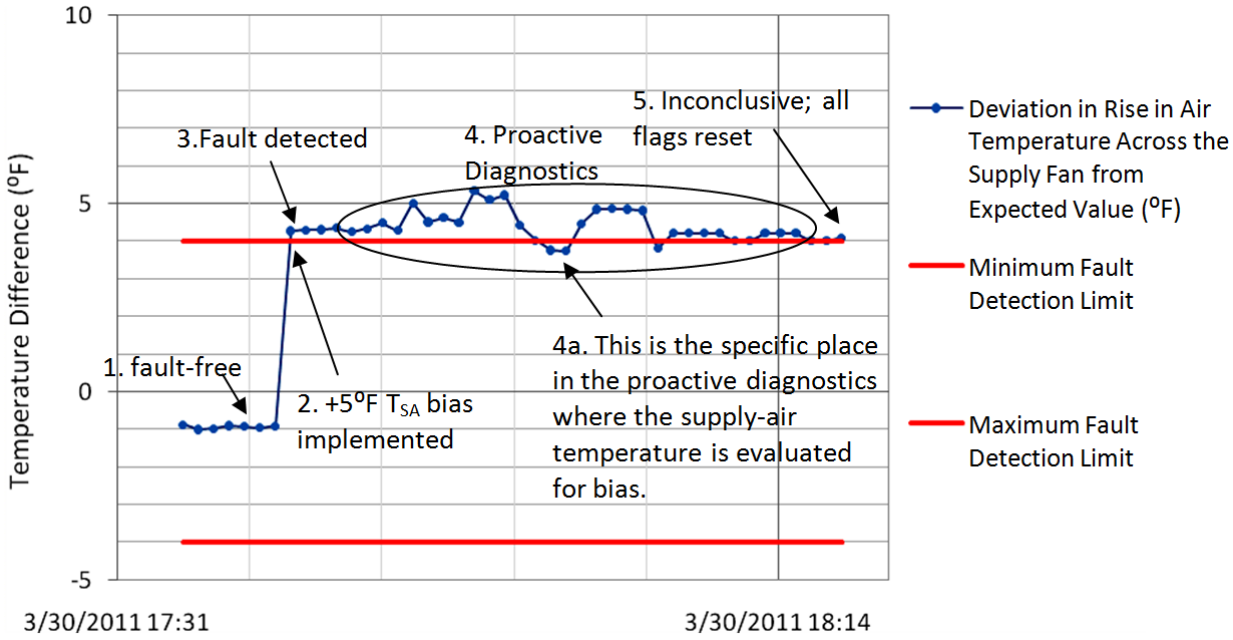

Figure 26 shows the time history of the deviation of the air temperature increase caused by fan heat rejection from its expected value based on the relationship found in Training 1, this time for a test for which all steps were completed successfully. The applied bias in Test 2 was +5°F, the same as in Test 1, but the temperature sensor tolerances were lowered to 1°F. With the lowered tolerances, the issue that arose in Test 1 did not arise in this test. After the proactive diagnostics, the program successfully determined that the fault was in the supply-air temperature sensor. The program then began the fault correction process, determined that the nature of the fault was a steady bias, and then averaged the bias over a period of several minutes, finally determining that the magnitude of the fault was 4.1°F. This correction is well within the tolerances of the sensors and can, therefore, be considered a correct recalibration of the supply-air temperature sensor.

Figure 26: Test 2 - Deviation of Fan Temperature Rise from Expected Training Value

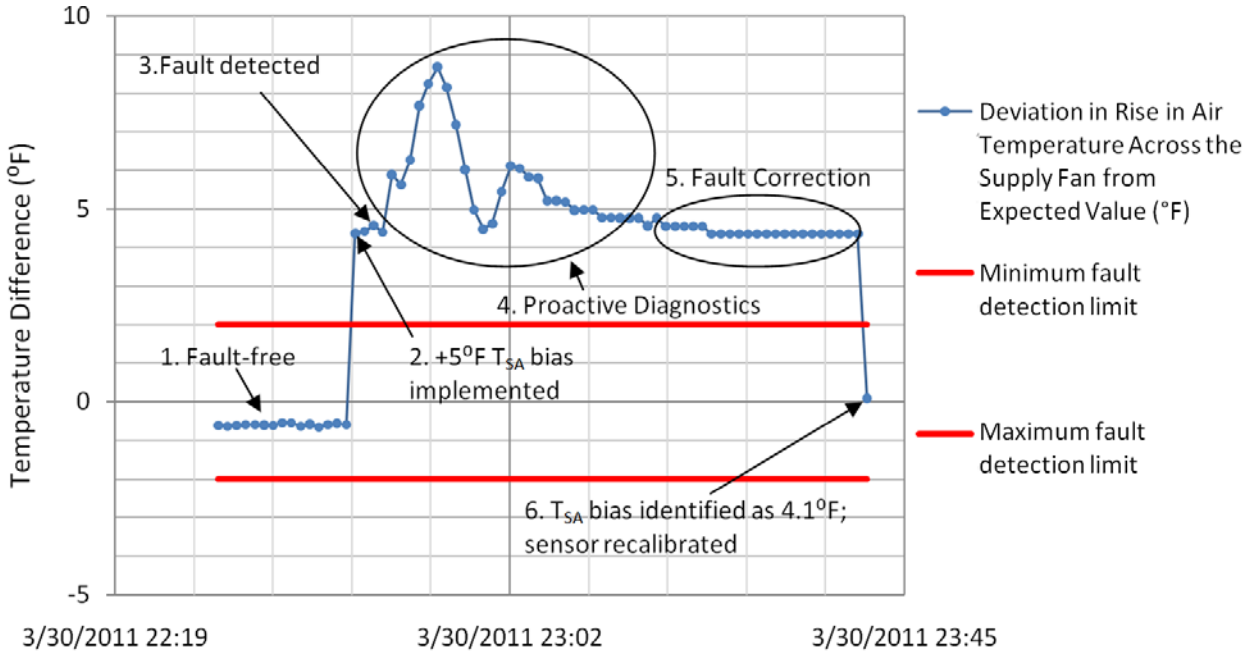

Plotting the time series of the same variable (i.e., the deviation of the air temperature increase caused by fan heat rejection from its expected value) during Test 3 in Figure 27 shows the results of the same fault correction process, this time for a +8^{0}F supply-air temperature sensor bias. This test illustrates that an increased severity (magnitude) of the fault has the same practical effect as lowering the tolerances for fault detection. If the tolerances were lowered too far, however, the rate of false fault detection would increase substantially. In Test 3, the fault was identified correctly as a supply-air bias fault with a magnitude of 6.63^{0}F and corrected.

Tests 4 through 6 examined detection, diagnosis and correction of biases in the measurements by the supply-air flow-rate meter. Two levels of fault severity were tested, a bias of +10% of the full speed air-flow rate (132 cfm) and a bias of +20% of the full speed air-flow rate (265 cfm). Tests 4 and 5 were each at +20% severity.

The algorithms easily detected and isolated the Test 4 fault because the value of the supply fan control signal, U_{SF}, was well above the range of $U_{SF,cal}$ [the expected value of U_{SF} obtained from the empirical relation between the normal supply-air flow rate (V_S) and U_{SF} developed in Training 1]. As shown in Table 5, the tolerance for the supply-fan control signal $U_{SF,tol}$ was set to 10. Therefore, U_{SF} must deviate from $U_{SF,cal}$ by at least 10 for a bias fault to be detected. In Test 4, after detection of a fault, the proactive diagnostics successfully isolated the fault to the supply-air flow meter; however, the fault was incorrectly characterized as caused by an erratic sensor rather than a steady bias in the flow meter measurements.

During the fault correction process, the readings from the faulty sensor are monitored for a period of 15 minutes under controlled conditions to evaluate whether they are relatively constant. When a relatively constant bias persists for 15 minutes, the algorithm deems the fault condition a biased sensor, rather than acting erratic one.

Figure 27: Test 3 - Deviation of Fan Temperature Rise from Expected Training Value

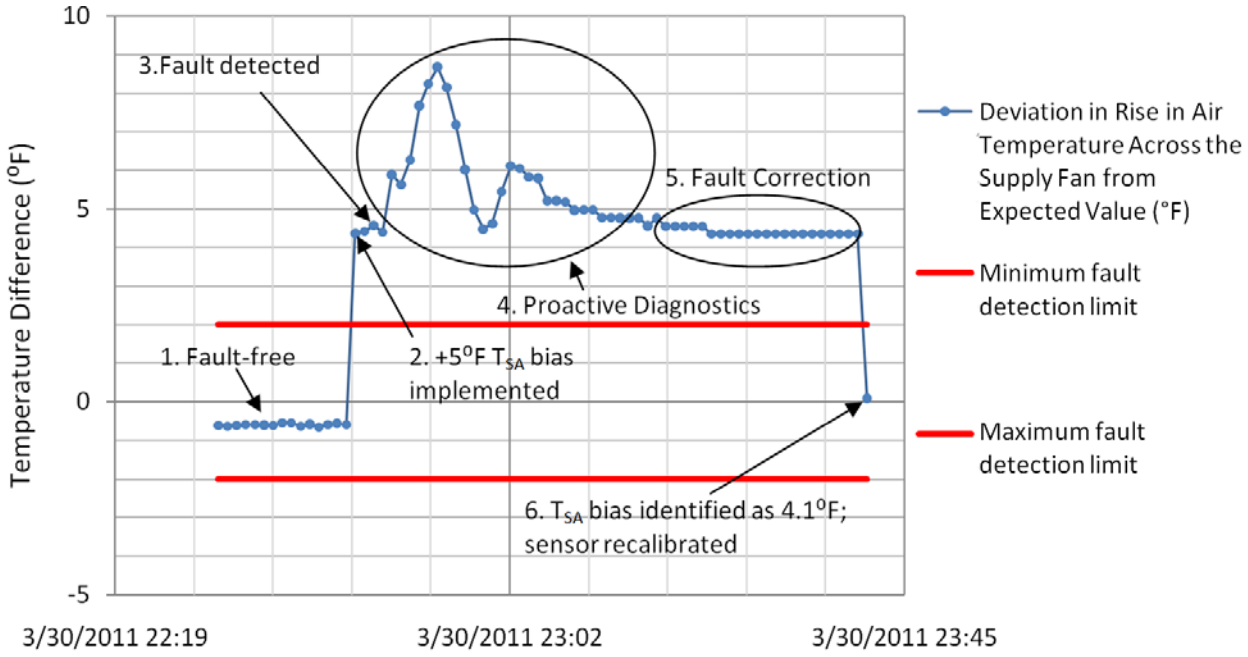

A statistical test is used to determine whether the sensor is behaving erratically or not. The sensor is behaving erratically unless two criteria are met: 1) the standard deviation of readings from the same sensor over the 15-minute period must be below a specified threshold (discussed later) and 2) no more than 10% of all data points collected during the 15-minute period can lie more than 2 standard deviations from the mean (randomly distributed data should have about 5%). The threshold for the standard deviation specified for Test 4 was 20 cfm. The observed standard deviation of the data equaled 47 cfm, thus exceeding the threshold, so that the sensor behavior as consider erratic and not a constant bias.

The value of the threshold for the standard deviation was chosen somewhat arbitrarily based on limited past tests. Both the uncertainty in measurements by the flow station (sensor) and variations in the flow rate contribute to variations in the flow rate with time. The air-flow rate through a duct may not be entirely steady, and small variations may affect the measured flow rate at the instants that measurements are made (caused, for example, by vortices and recirculation). Thus, knowing the uncertainty of the sensor under ideal conditions is likely insufficient information to choose an effective standard deviation threshold. This threshold is thus one that should be set empirically, based on tests or experience with a known, properly working sensor. We reset the standard deviation threshold to 60 for Tests 5 and 6.

With the standard deviation threshold changed, the algorithms for all steps executed successfully in Test 5. Figure 28 shows the process during the passive diagnostics that led to fault detection. Here, the values of $U_{SF,cal}$ calculated from measured values of air-flow rate and the relationship established during training, track the actual supply-fan control signal U_{SF} closely until the fault is implemented, after which $U_{SF,cal}$ is about 20 higher. The solid red lines in the graph show the limits for fault detection, which $U_{SF,cal}$ is clearly within before the fault

occurs and above the upper limit following fault implementation (the black line shows the implementation of the bias for which the scale is shown on the right axis).

Figure 28: Test 5 - Passive Diagnostics - U_{SF} versus $U_{SF,cal}$

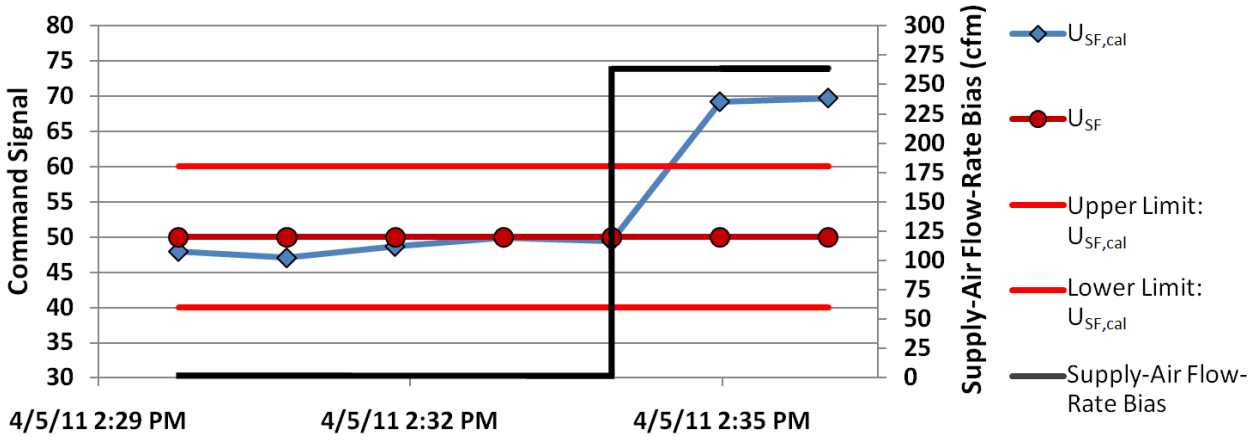

During the proactive diagnostics, the critical test that traces the fault to the supply-air flow meter is shown in Figure 29. The test stipulates that for the fault to be characterized as a supply-air flow-meter fault, the flow rates measured at the VAV terminal boxes must all be above or all be below the measured air-handler supply-air flow rate, with an additional threshold that serves as a margin of error in this calculation (which was set 20 cfm). The flow rates measured at each VAV terminal box are adjusted higher to account for the "leakage flow" characterized during the Training 2. The leakage flow is the average flow rate that leaks from the ductwork and any of the other dampers when one damper in the VAV box network is fully open and the rest are fully closed. During this proactive test, the damper of each VAV box is sequentially opened while the rest are closed to compare their individual flow rates under these conditions to the supply-air flow rate measured at the air handler. If the VAV-box flow meters are working properly, then the actual flow rate at the open VAV box during this test should equal the air-handler flow rate minus the leakage flow rate measured during Training 2. Figure 29 shows that each measured supply-air flow rate is at least 235 cfm greater than sum of the VAV-box and leakage flow rates, indicating that the supply-air flow meter is faulty (reading high).

With the standard deviation threshold raised for the fault correction process, there was no problem correctly isolating and then correcting the fault. The 265 cfm bias was characterized as a 287 cfm bias, which was a very close correction (within 8.5% of the actual bias).

Figure 30 shows measurements during the passive diagnostics for Test 6 at a fault severity of +10% of full speed flow rate. This fault, much like the fault for Test 1, is right at the limits of fault detection. As shown in the figure, the fault was detected after $U_{SF,cal}$ barely rose above the upper limit for fault detection.

Figure 29: Test 5 - Proactive Diagnostics - VAV versus Supply Flow Rate

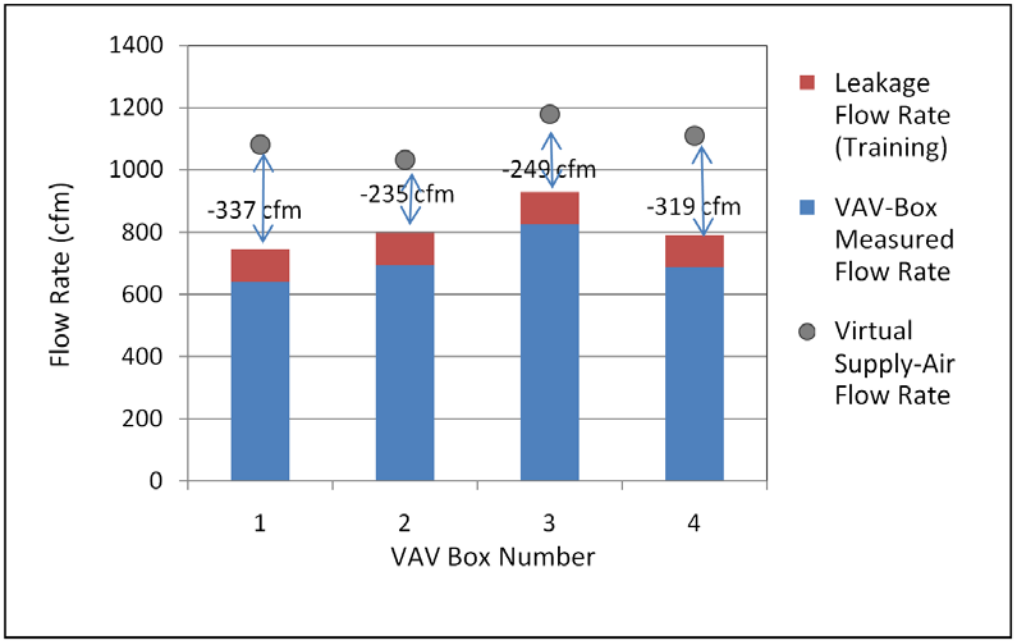

Figure 30: Test 6- Passive Diagnostics- U_{SF} versus $U_{SF,cal}$

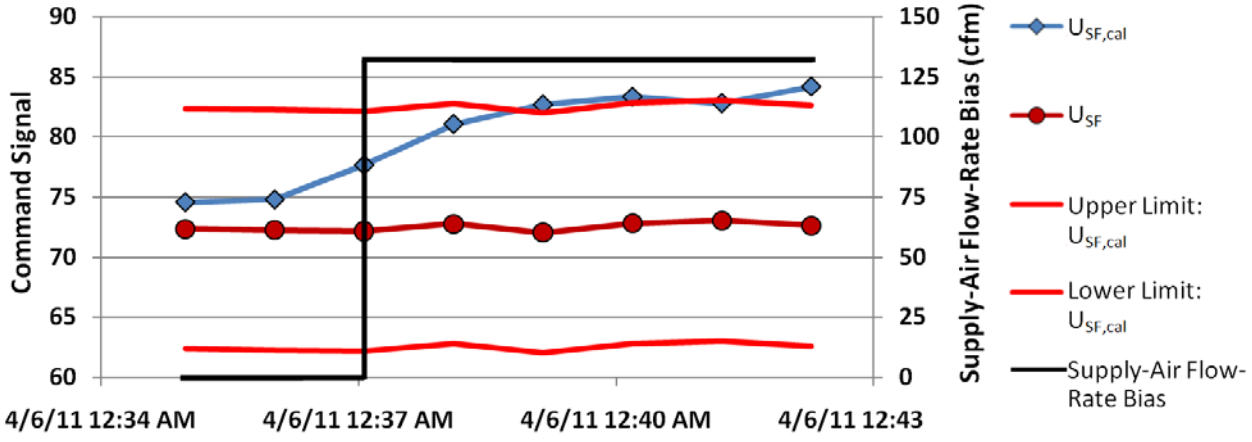

Analogous to the situation in Test 1, during the proactive diagnostics in Test 6, the variable intended to indicate the presence of the fault was only slightly above the upper limit for detection in the passive diagnostics and slightly below the lower limit for diagnosis in the proactive diagnostics. For correct diagnosis of the supply-air flow meter fault, the sum of the measured flow rate and the leakage flow rate must be above the measured air-handler supply-air flow rate plus the 20-cfm threshold or below the measured air-handler supply-air flow rate minus the 20-cfm threshold of the supply-air flow rate for all VAV boxes. For Test 6, the

measured flow rates for all the boxes but one are much more than 20 cfm below the measured air-handler supply-air flow rate (see Figure 31). Box #3, however, only reads 17 cfm below the measured supply-air flow rate. The algorithm concludes, therefore, that the supply-fan belt is slipping, the supply-fan efficiency has decreased, or VAV dampers are stuck. These faults are indistinguishable from one another in the current set of algorithms. As a result, the proactive diagnostic algorithm reached the wrong conclusion.

Figure 31: Test 6 - Proactive Diagnostics VAV versus Supply-air Flow Rate

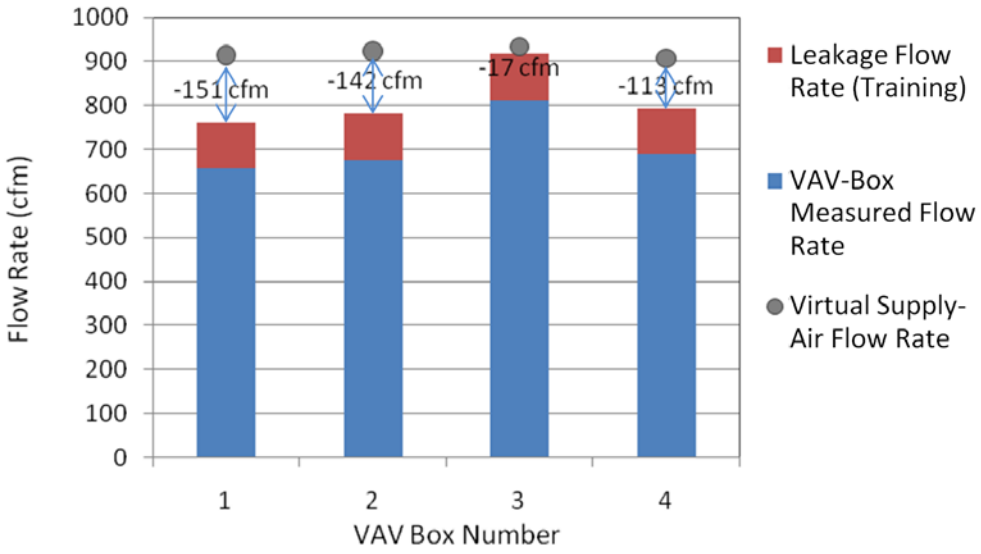

Recall that in Test 1, the algorithm reported the result as "inconclusive," and the algorithm returned the process to the passive diagnostics to start over. This is preferable to an incorrect conclusion as in Test 6, when the fault severity is borderline. The inclusive result was reached in Test 1 because the logical structure of the algorithms provided for unique tests for all possible faults. The logical structure for identifying the fault with the supply-air flow measurement, in contrast, is a "process of elimination," wherein if the fault must be A or B, and we determine that fault A for which we can directly test has not occurred, then the fault that occurred must be fault B. As a result, Test 6 reveals a weakness in the approach used for isolating the supply-air flow-rate sensor fault.

Without adding sensors to the VAV system (a constraint imposed by the technical team to reduce the incremental cost of implementing self-correcting capabilities), not much can be done about the rigor of the logic. There are, however, steps that can be taken to better ensure that supply-air flow-meter faults are correctly isolated. One is to set the fault detection thresholds so that they are higher than the fault diagnostic thresholds. Another is to redesign the training process for the leakage flow rates. Rather than assuming that the leakage flow is identical for all VAV boxes, the system could be trained to determine a unique leakage flow rate for each VAV box. Referring to Figure 31, perhaps the leakage flow rate is much lower when VAV Box 3 is fully open and the others are completely closed.

CHAPTER 4:
Economic and Impact Assessment

Many faults affecting the energy efficiency and performance of HVAC systems go undetected and uncorrected, often for long periods of time. Even when faults are detected and properly diagnosed, it is common for faults to persist because building operations staff do not find the time to address many of these faults, or HVAC service technicians do not receive approval from building owners to complete the required service or repair. Self-correcting controls could automatically correct many of these faults by reconfiguring controls and recalibrating devices, and thus enable the system to maintain performance efficiency. To estimate the potential energy and economic impacts of deploying self-correcting controls, we first estimate HVAC system-level savings (on average) and then multiply the savings by the potential number of systems impacted. Cost savings and environmental benefits are then derived from the estimated energy savings. To appropriately capture the persistent savings from controls that continually self-correct operational faults, the savings are estimated over a 15-year period based on forecasted building stock and energy price estimates developed by the California Energy Commission (CEC).

Technical and Market Potential

Based on published reports, savings between 10% and 30% are generally achievable by correcting operation problems. It is reasonable to assume that systems retrofit with robust self-correcting controls could achieve average HVAC energy savings of 15% over common operation conditions for applicable systems over the lifetime of the system (Mills 2009, Moore et al. 2008, Roth et al. 2005, Tso et al. 2007).

The targeted market will include built-up, central HVAC systems with a longer-term market potential targeting packaged HVAC systems. To determine the energy savings potential for these targeted systems, the energy consumed by various HVAC systems was calculated based on equipment shares derived from California Commercial End-Use Survey (CEUS) data (Itron 2006).[3] The CEUS survey queries provided information on equipment shares by building stock and climate zone as well energy consumption by end use. California commercial building stock forecasts were taken from the California Energy Commission's (CEC's) most recent energy forecast (CEC 2009). Equipment shares by building type and building stock forecasts were then input into the PNNL-developed Building Energy Analysis Modeling System (BEAMS)[4] to derive consumption by equipment type (Elliott et al. 2004).

Overall, the total energy used by both built-up and packaged systems to heat, cool , and ventilate commercial buildings in California is estimated to make up about one-quarter of the total delivered energy use in the overall commercial sector and just over three-quarters of the total delivered commercial HVAC energy use. Figure 33 provides a diagram identifying the

[3] CEUS data query received in Excel format from Mark Ciminelli, Senior Mechanical Engineer, California State Demand Analysis Office (10/13/2010).

[4] Chapter 2 of referenced report (Elliott et al. 2004) provides a detailed description of "BESET" model, which has since been renamed as "BEAMS."

energy use targeted by self-correcting HVAC controls. The energy use includes both natural gas and electric delivered energy consumption in trillions of British thermal units (TBtus). The initial target, which focuses on built-up systems, only accounts for about 17 % of total HVAC energy use in commercial buildings; however, these self-correcting systems will be available for retrofit, enabling near-term deployment into the existing building stock. Packaged systems make up a much larger portion of the total HVAC delivered energy use (60%); however, the current set of self-correcting controls has not yet been tested or demonstrated on packaged systems, so deployment into this market would likely be further in the future.

Figure 32: Target Market for Self-Correcting Controls (Delivered TBtus)

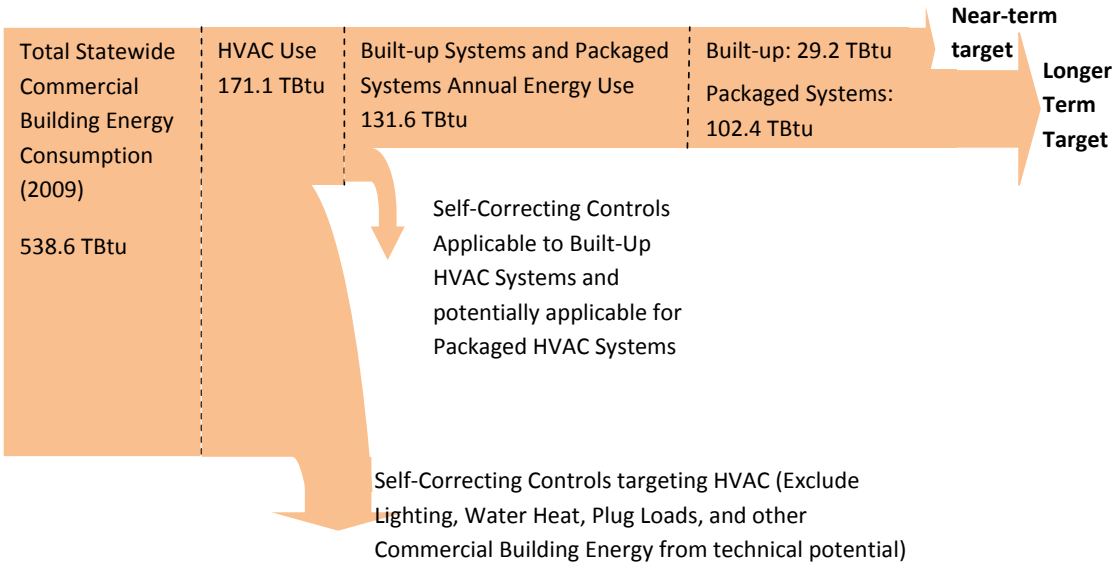

Methodology

The benefit estimates for self-correcting controls are estimated with PNNL's Building Energy Analysis Modeling System (BEAMS). BEAMS is a bottom-up accounting model that compares baseline energy use against specific energy-efficient technologies or energy saving programs (Elliott et al. 2004). The BEAMS model baseline was calibrated to represent the California commercial building energy market. The underlying building stock assumptions and forecast are based on the most recent CEC energy forecast (CEC 2009), while HVAC equipment market shares by building type are based on CEUS survey results (Itron 2006). Average equipment efficiencies were drawn primarily from the Department of Energy's (DOE's) National Energy Modeling System (NEMS) input assumptions (EIA 2010). The baseline also includes heating and cooling end-use loads representing the baseline heating and cooling energy use per square foot. To appropriately represent the savings in a particular sector, the baseline includes commercial building end-use loads developed for specific building types (e.g., education, large office, etc.) as well as by vintage for two encompassing California climate zones. End-use loads were derived from the Facility Energy Decision System (FEDS) to reflect current energy technology and consumption behavior (PNNL 2008).

The market penetration over time is developed based on market diffusion curves developed by PNNL, which are based on a Bass diffusion model (Bass 1969) for various building HVAC

technologies (Elliott et al. 2004[5]). Bass was the first to suggest the "S" curve or logistic functional form for the market diffusion of new products, and his concepts are still widely employed in the marketing discipline today. The model development and empirical analysis were designed to generate more credible predictions of the adoption process of energy-efficiency technologies in the buildings sector. The timeframe for this study is limited to a 15-year period.

Built-up System Savings

The initial set of self-correction methods and algorithms developed as part of this project are being tested and demonstrated on built-up HVAC systems. Built-up HVAC systems are characterized as central HVAC systems that are custom-designed for a building. Chillers and boilers make up the source components for the vast majority of the built-up systems in the California commercial building stock; however, a small percentage of the built-up systems are supplied with other HVAC source components (e.g., central air-conditioning and gas furnaces). The shares of built-up systems are identified with CEUS data queries to characterize the market potential and market penetration of self-correcting controls into this market.

Two deployment paths were considered related to the deployment of self-correcting controls into the built-up HVAC market:

> Deployment Path 1: Deployment of self-correcting controls as software code in an energy management and control system or building automations systems (BAS) in commercial buildings or as a third-party software connected to a BAS; and
> Deployment Path 2: Deployment by integrating self-correcting code into distributed field panels or device controllers.

Although BAS are found in relatively few buildings overall (5% of buildings encompassing approximately 17% of commercial floor space), they are much more prevalent in buildings that have built-up systems. Based on data queries from the Energy Information Administration (EIA) Commercial Buildings Energy Consumption Survey (CBECS), it is estimated that approximately 50% to 70% of commercial floor space served with built-up systems in California is equipped with building automation systems (EIA 2003). Deployment through a BAS system would, therefore, provide significant opportunities to penetrate buildings with a newly installed BAS; but more importantly, it would also provide opportunities to retrofit and impact a large fraction of the existing building stock because these systems could be retrofit more easily and cost effectively with self-correcting controls. The second deployment path, "Deployment by integrating self-correcting code into distributed field panels or device controllers " would also provide opportunities to reduce energy use within the existing building stock; however, the opportunity for retrofit would more likely come as system components are retired and changed out or upgraded, which would be a much slower process.

To assess the energy market and economic impact of self-correcting controls in the built-up market, it was assumed that a very aggressive market deployment program could achieve 40%

[5] See Chapter 3, "Technology Diffusion Models – Application to Selected Energy-Efficient Products for Buildings," of Elliott et al. for more information on development of diffusion models. Sources for HVAC technology data and conclusions include Census of Manufacturers, Gas Appliance Manufacturers Association (GAMA) [Srinivasan & Mason (1986); Brown et al. (1989); Mahajan, Mason, and Srinivasan (1986)].

market penetration in the built-up HVAC market 15 years after the initial date of commercialization by focusing on deployment through BAS. It is also assumed that an additional 20% of the built-up HVAC stock that is new or is turned over during a 15-year period could be impacted with self-correcting controls through one or both of the previously described deployment paths. Table 9 provides the market diffusion estimates over a 15-year period for the previously described "aggressive" deployment, which is referred to as the "High" market penetration scenario. In addition, Table 9 provides market diffusion estimates for the "Moderate" market penetration scenario and for "Low" market penetration assumptions.

Table 8: Market Diffusion and Energy Performance Assumptions for Built-up Systems

Year	Percentage of Built-up systems/stock (targeting buildings with BAS)			Percentage of new and turnover equipment (source components for built-up systems)			HVAC Energy Reduction per unit
	Low	Moderate	High	Low	Moderate	High	
1	0.5	0.8	1.0	0.3	0.4	0.5	15%
2	1.2	1.8	2.4	0.6	0.9	1.2	15%
3	2.1	3.1	4.1	1.0	1.6	2.1	15%
4	3.2	4.7	6.3	1.6	2.4	3.2	15%
5	4.5	6.7	9.0	2.2	3.4	4.5	15%
6	6.0	9.1	12.1	3.0	4.5	6.0	15%
7	7.8	11.7	15.6	3.9	5.8	7.8	15%
8	9.7	14.5	19.4	4.8	7.3	9.7	15%
9	11.6	17.4	23.2	5.8	8.7	11.6	15%
10	13.5	20.2	27.0	6.7	10.1	13.5	15%
11	15.2	22.8	30.5	7.6	11.4	15.2	15%
12	16.8	25.1	33.5	8.4	12.6	16.8	15%
13	18.1	27.1	36.1	9.0	13.6	18.1	15%
14	19.1	28.7	38.3	9.6	14.4	19.1	15%
15	20.0	30.0	40.0	10.0	15.0	20.0	15%

Assuming an average HVAC energy reduction of 15% by year 15 and the market diffusion described in Table 9, the deployment of self-correcting controls in the built-up HVAC system market produces a year 15 statewide annual savings of 1.2 TBtu, under "Low" market penetration assumptions, 1.8 TBtu under "Moderate" penetration assumptions, and 2.4 TBtu under "High" penetration assumptions (see Figure 34).

Although savings are initially relatively modest, they increase substantially over time. The increase results from both the increasing market penetration as well as the savings that persists over time. The persistence of savings is especially important when evaluating self-correcting controls because a fundamental characteristic of these measures is that they sustain peak performance and efficiency, which has been found to be difficult for many commercial building energy-efficient technologies, designs, and measures.

In terms of specific end uses and fuel sources, most of the delivered energy savings generated from self-correcting controls in built-up systems are in the form of gas heating reductions. Figure 35 provides the breakout, over time, of the savings by end use and fuel source for the

Figure 33: Self-Correcting Annual Energy Savings for Built-up Systems by Market Penetration Scenario

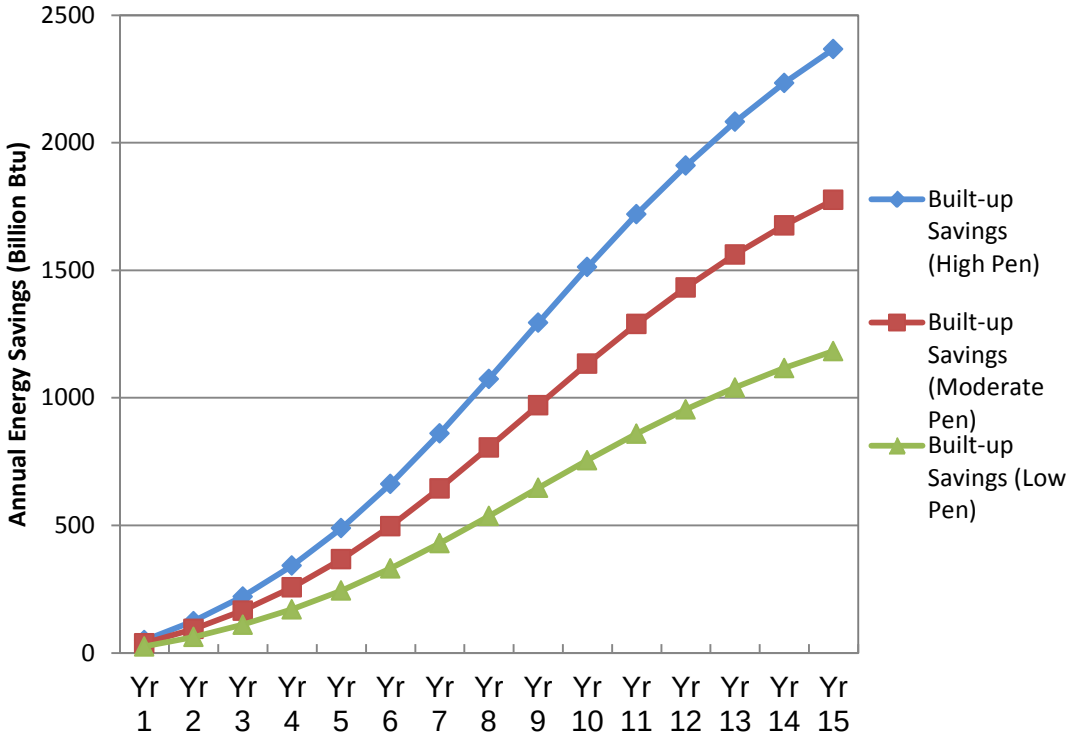

deployment of self-correcting controls into built-up systems, assuming the "High" penetration scenario.

Figure 34: Built-up Annual Energy Savings by End- Use and Fuel Source (under the "High" market penetration scenario)

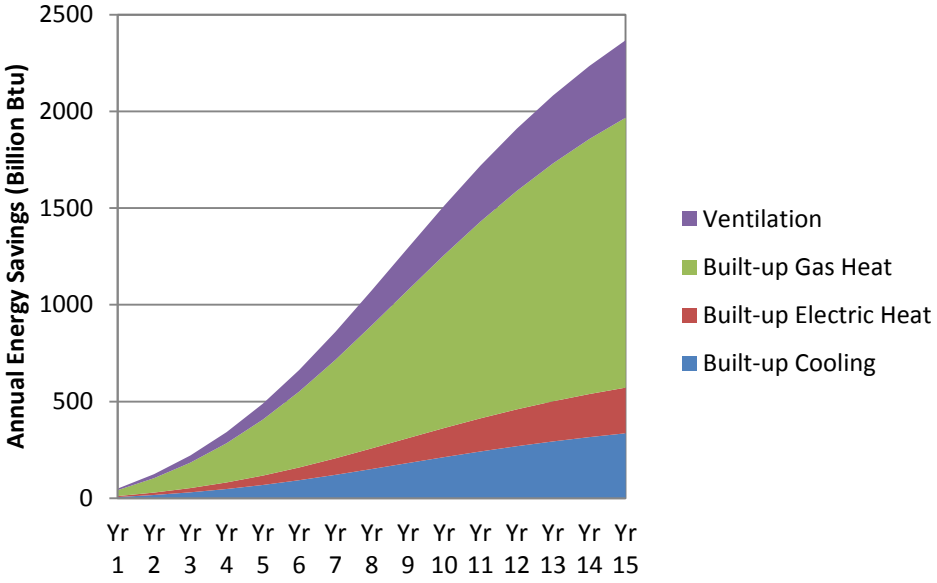

Built-up system savings from self-correcting controls are concentrated in a few building types, with the miscellaneous building category (e.g., public assembly, religious, etc.), education, and large offices[6] making up just over 85% of the savings (see Figure 36) 10 years after the initial deployment. Health care facilities make up an addition 11% of the savings.

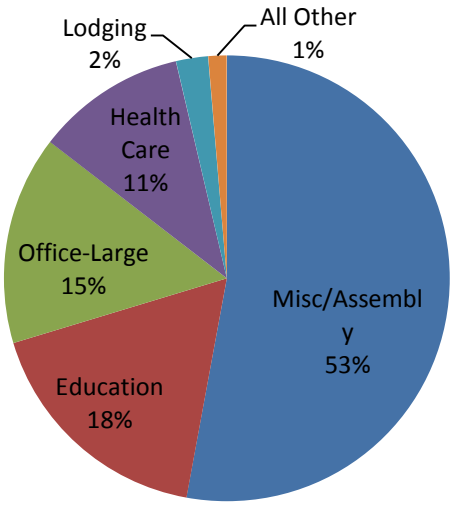

Figure 35: Percent of Savings in Built-up Systems by Building Type

Packaged System Savings

Although the self-correcting controls developed as part of this project have not been directly tested or demonstrated on packaged systems, it is believed that the algorithms developed for built-up systems could be tailored to packaged systems to achieve similar performance benefits. Packaged systems are the most common HVAC systems in commercial buildings and make up 60% of the total HVAC energy consumption in California. Thus, any measure that improves the performance of packaged systems, in general, could have significant energy reduction impacts. Because packaged systems tend to be serviced less than built-up systems and are less likely to be affiliated with a BAS, there would likely be fewer opportunities to retrofit existing packaged systems with self-correcting controls. The pathway for deployment of self-correcting controls would therefore more likely occur at the equipment production level for packaged systems. There are five well known manufacturers of commercial HVAC equipment that dominate the market: Carrier, Lennox, McQuay, Trane, and York. Based on a 2005 Northwest Energy Efficiency Alliance (NEEA) study, the "Big Three" manufacturers for packaged heating and cooling equipment used in the Pacific Northwest are Trane, Carrier, and Lennox, where Trane is estimated to have 50% of the market share, followed by Carrier (30%), and Lennox (15%) (NEEA 2005). Other manufacturers, mainly York, are estimated to have 5% of the packaged HVAC commercial market share. Assuming that the California HVAC market is similar to the Northwest and low-cost self-correcting controls were available and could be integrated into a packaged system during fabrication, only one or two companies would need to integrate these capabilities into their systems to provide a sizable impact on HVAC energy consumption.

[6] "Large offices" are defined as office buildings equal to or greater than 30,000 square feet.

To assess the energy and economic impacts of self-correcting controls in the packaged system market, it was assumed that an aggressive market deployment program could achieve 40% of the packaged system HVAC stock that are new or replacement units during a 15-year period.[7] This would not include the fraction of existing packaged systems that could potentially be retrofit to incorporate self-correcting controls. Table 10 provides the market diffusion estimates for a "Low," "Moderate," and "High" market penetration scenarios over a 15-year period.

As shown in Figure 37, even while only penetrating into new equipment, the energy savings potential for deploying self-correcting controls into packaged systems is significant because of the prevalence of these systems. By year 15, annual savings reach 3.8 TBtus under the scenario with "High" market penetration assumptions, 2.8 TBtus under the "Moderate" market penetration scenario and 1.9 TBTus under the "Low" market penetration assumptions.

The savings generated from self-correcting controls deployed in packaged systems comes primarily in the form of natural gas heat savings and cooling savings. Figure 38 provides the breakout, over time, of the savings by end use and fuel source for the deployment of self-correcting controls into packaged systems, assuming the "High" penetration scenario.

Table 9: Market Diffusion and Energy Performance Assumptions for Packaged Systems

Year	Percentage of new and turnover package system equipment			HVAC Energy Reduction per unit
	Low	Moderate	High	
1	0.5	0.8	1.0	15%
2	1.2	1.8	2.4	15%
3	2.1	3.1	4.1	15%
4	3.2	4.7	6.3	15%
5	4.5	6.7	9.0	15%
6	6.0	9.1	12.1	15%
7	7.8	11.7	15.6	15%
8	9.7	14.5	19.4	15%
9	11.6	17.4	23.2	15%
10	13.5	20.2	27.0	15%
11	15.2	22.8	30.5	15%
12	16.8	25.1	33.5	15%
13	18.1	27.1	36.1	15%
14	19.1	28.7	38.3	15%
15	20.0	30.0	40.0	15%

[7] Although packaged system impacts would not be expected in the near-term, the impacts for a 15-year period are projected during the same 15-year period as the built-up systems for convenience and to coordinate with the CEC building and price forecasts.

Figure 36: Self-Correcting Annual Energy Savings for Packaged Systems by Market Penetration Scenario

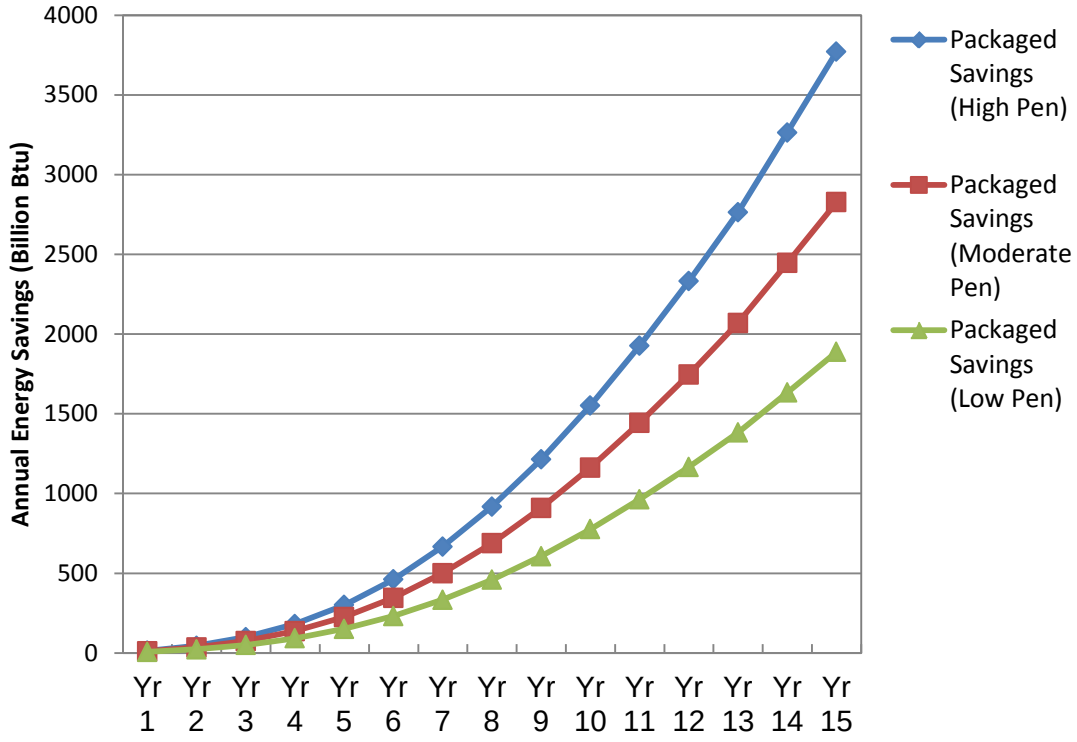

Figure 37: Packaged System Annual Energy Savings by End Use and Fuel Source (under aggressive market penetration scenario)

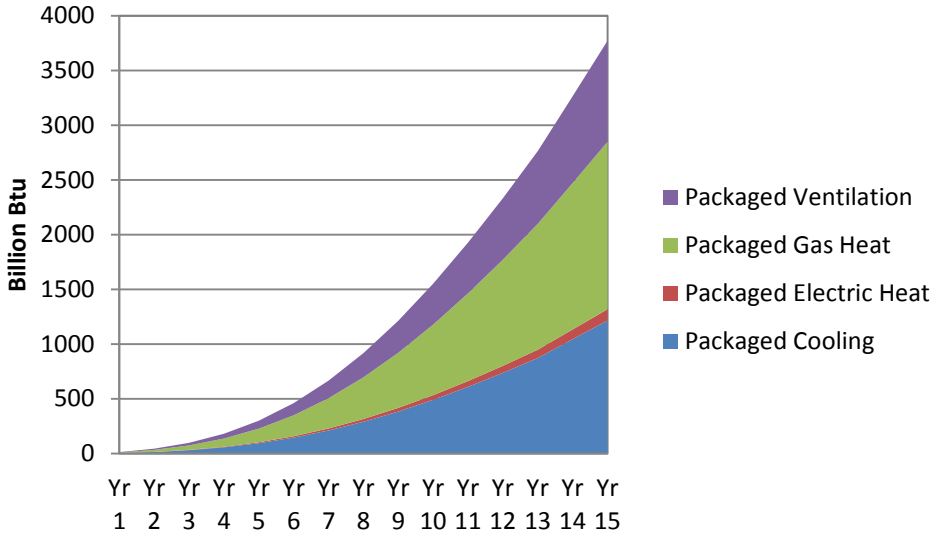

Relative to the built-up system savings, the packaged system savings are spread more evenly amongst all building types; however, approximately two-thirds of the savings are concentrated

in retail buildings, warehouses, education and miscellaneous building categories. Figure 39 provides the savings percentages by building type for packaged system savings.

Figure 38: Percent of Savings in Packaged Systems by Building Type

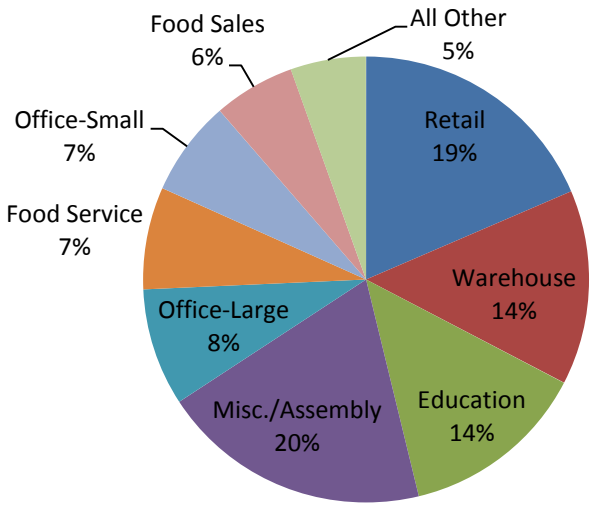

Total Impacts on California Market

Overall, the deployment of self-correcting controls in both built-up and packaged systems could noticeably reduce California HVAC energy consumption over time. Figure 40 presents the annual savings projections by system type, while Figure 41 presents the savings total if deployment were to occur in built-up and packaged systems assuming aggressive deployment (i.e., "High" market penetration assumptions). As shown in Figure 40, built-up system savings are initially greater than packaged system savings as a result of the retrofit potential of these systems into existing building stock. In the longer-term, however, the deployment of self-correcting controls into packaged systems becomes relatively greater as stock turns over because of the large quantity of these systems in the commercial buildings market.

As shown in Figure 41, the combined annual delivered energy savings of deploying self-correcting controls into both packaged and built-up systems is 3 TBtu after 10 years under the aggressive or "High" market penetration scenario. These annual savings increase to 6.1 TBtu/year at year 15 (i.e., 15 years after the date of commercialization). This savings would equate to an approximate 3% to 4% overall reduction in commercial HVAC consumption in California over a 15-year period.

Figure 39: Self-Correcting Annual Energy Savings by System Type with Aggressive Market Deployment Assumptions (i.e., "High Pen")

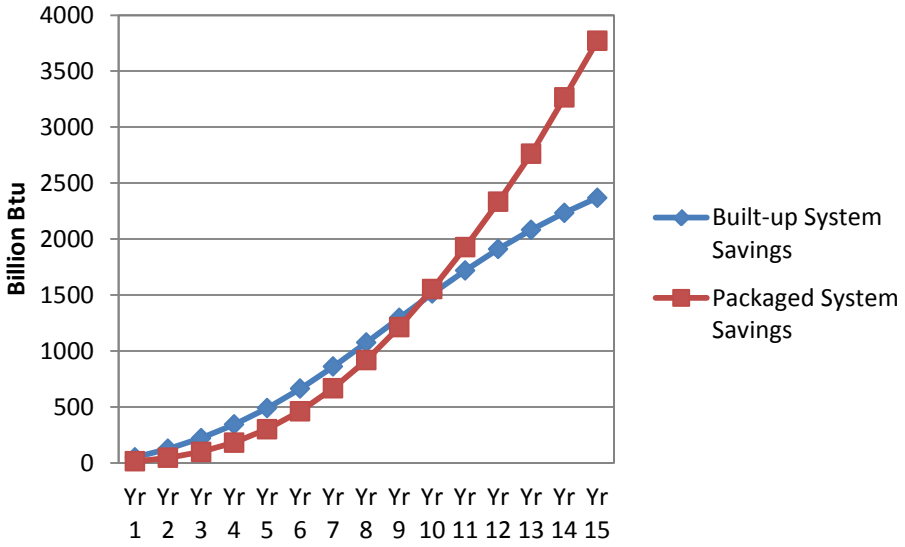

Figure 40: Total Delivered Annual Energy Savings (both electric and natural gas) with Deployment into both Built-up and Packaged Systems (High Market Penetration Scenario)

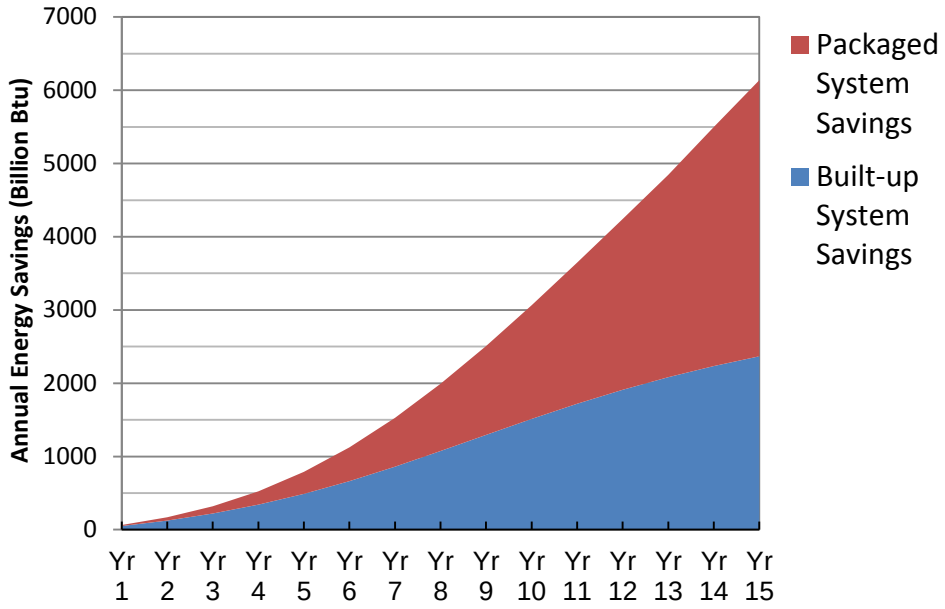

Economic Impact

The energy cost savings associated with the energy savings presented in Figure 41 are shown in Figure 42. Cost savings are derived by multiplying the savings (by energy type) by the delivered energy price, which are forecasted by the CEC[8]. In the near-term (year 5), the self-

[8] Prices forecasted by CEC out to the year 2020. Beyond 10 years, prices were held constant at 2020 prices.

correcting controls deployment would result in a relatively modest annual savings of between $8 and $11 million for each system type in which deployment occurs. An aggressive deployment into both built-up systems and packaged systems could yield an annual cost savings of approximately $84 million 10 years after commercialization and $163 million 15 years after the technologies are commercialized.

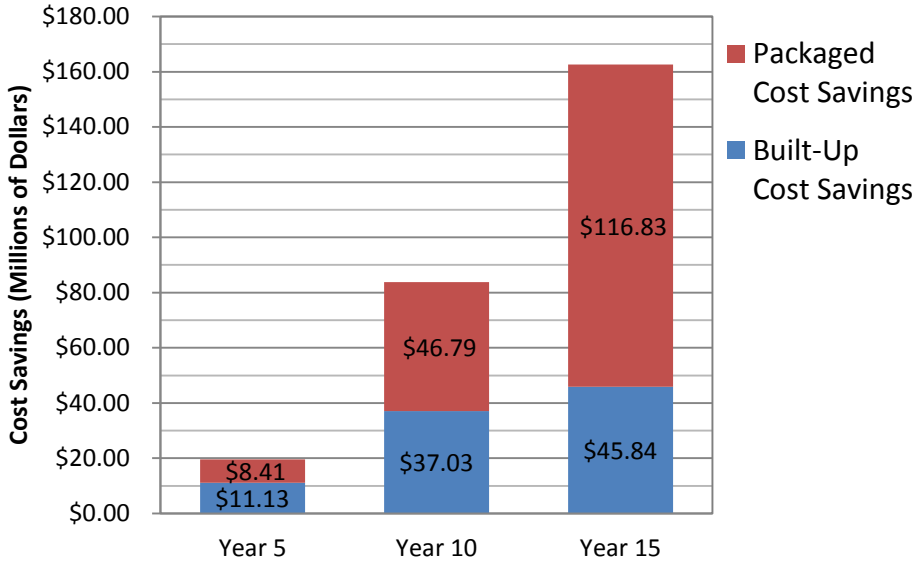

Figure 41: Annual Forecasted Energy Cost Savings by System Type

Environmental Impacts

The importance of reducing carbon dioxide (CO_2) emissions has increased significantly in recent years. The estimate of CO_2 emission reductions associated with the energy savings from self-correcting controls is based on an average CO_2 emissions avoidance factor per unit of energy consumption for the state of California[9]. The CO_2 emissions reductions are directly related to the energy savings presented in Figure 41 and the respective fuel source associated with the energy savings.

It was estimated that approximately 7,000 to 10,000 metric tons of carbon equivalent (MMTCE) would be avoided annually by deploying self-correcting controls in either built-up or packaged systems (see Figure 43). Approximately 65,000 MMTCE could be avoided annually with an aggressive deployment of self-correcting measures in both built-up and packaged systems in 10 years from the initial deployment of the controls, which would increases to annual carbon emission avoidance of approximately 131,000 MMTCE 15 years after the initial deployment.

[9] Emissions from electric usage are calculated using an average emissions rate for EPA's E-Grid subregion: WECC California (724.1201 lb/MWh), which are consistent with rates independently certified and registered each year by the California Climate Action Registry (see www.climateregistry.org) (EPA 2007).

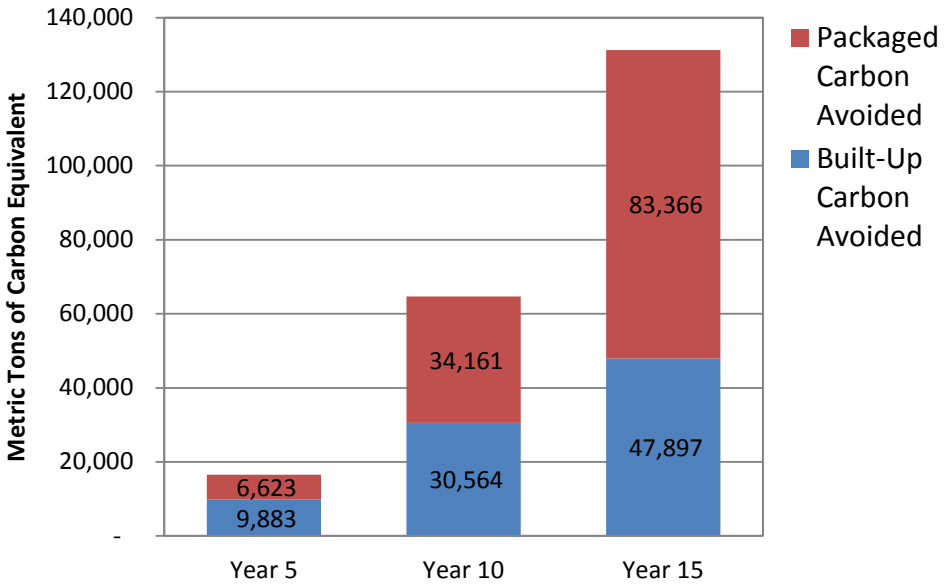

Figure 42: Annual Equivalent Carbon Dioxide Emissions Avoided by System Type (MMTCE)

CHAPTER 5:
Future Work

Proposed future work falls into three categories: 1) improved models and procedures for collecting training data, 2) completion of the full suite of tests necessary to validate the fault detection, diagnosis, and correction algorithms for the air handling (filter/fan/coil) and VAV sections, 3) integrating the self-correcting control algorithms with building automation systems other than the Johnson Controls Metasys®[10] used for the laboratory tests completed thus far, and 4) field testing the self-correcting control algorithms in operating commercial buildings.

Improved Training Models and Procedures

Each of the training algorithms requires modifications.

Training 1 requires only a slight modification. As noted in Chapter 3, no actuator response occurred for command signals under 25% for all dampers and valves in the laboratory system. The model for devices that respond in this manner should be revised to include a region for low values of command signals (e.g., less than 25%) for which no response occurs and a second region (e.g., 25% to 100%) in which the device (e.g., damper or fan) response increases with increasing command signal. A polynomial curve fit can then be used to capture the behavior in this second region. The value of the command signal at which the response becomes non-zero may differ among equipment, controllers and systems, so a step to identify this transition point needs to be added to the Training 1 process and algorithm.

As mentioned in Chapter 3, the leakage flow rate training (in Training 2) should be modified to the determine a leakage flow rate for each of the VAV boxes served by the air handler, rather than averaging the measured leakage flow rates to arrive at one leakage rate used for all VAV boxes.

Training 3 requires a more substantial revision. In hindsight, ΔT_{SM} is inadequate for tracking the performance of the cooling coil. As the difference between the mixed-air temperature and the chilled-water temperature changes, the achievable temperature drop across the cooling coil also changes. The heat exchanger effectiveness, which can be shown as equal to the air-side temperature drop across the cooling coil divided by the thermodynamic maximum temperature drop achievable by the air, would be a better variable for this purpose. For the cooling coil, that temperature drop would be the difference between the air temperature at the cooling-coil inlet and the chilled-water temperature (at the cooling-coil water inlet). The air-temperature leaving the cooling coil is not ordinarily measured; therefore, it must be estimated from the supply-air temperature accounting for the increase in temperature as the cooled air flows past the supply fan (ΔT_{SF}). The change in air temperature across the cooling coil is then estimated as the difference $T_{HC} - (T_{SA} - \Delta T_{SF}) = T_{HC} - T_{SA} + \Delta T_{SF}$, where T_{HC} is the air temperature leaving the heating coil but before entering the cooling coil (see Figure 1 for the locations of the sensors). Thus, the cooling-coil effectiveness (ε_{CC}) is given in terms of commonly available sensors by

[10] Metasys is a registered trademark of Johnson Controls, Inc.

$$\varepsilon_{CC} = \frac{T_{HC} - T_{SA} + \Delta T_{SF}}{T_{HC} - T_{CW}}.$$

When a heating coil is not present, the temperature entering the cooling oil can be taken as the mixed-air temperature, T_{MA}.

Figure 32 shows what Training 3 data from Figure 24 look like when the dependent variable plotted is ε_{CC}, rather than ΔT_{SM}. The relationships in Figure 32 and their dependence on the cooling-coil valve signal, U_{CC}, are much clearer than those shown in Figure 24. As U_{CC} is increased, E_{CC} increases. at first very quickly, then saturating at higher values of $U_{CC.}$

Figure 43: "Cooling Coil Effectiveness" from Training 2 Data

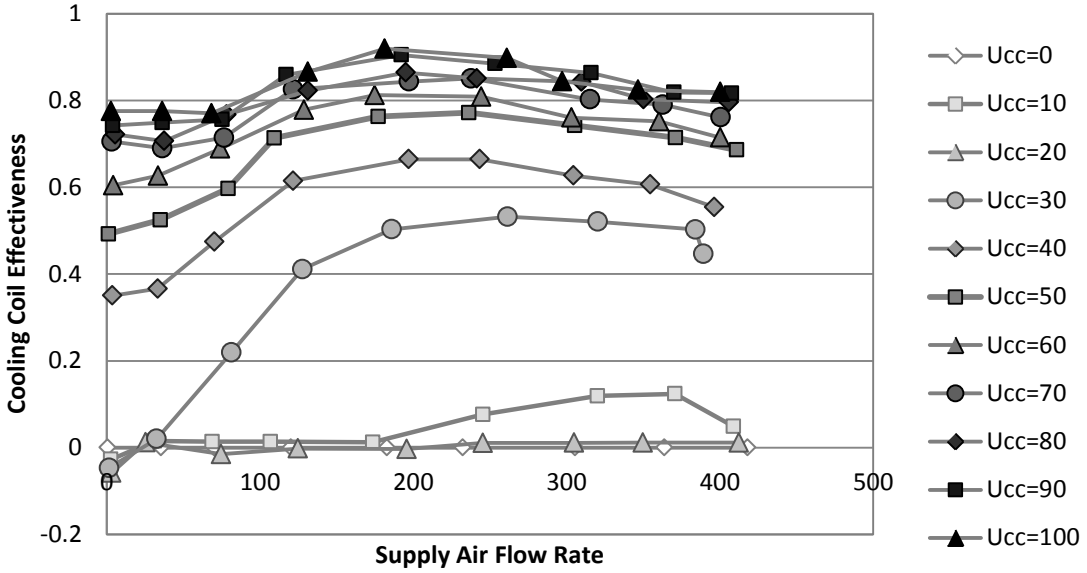

The model for Training 3 also needs to be corrected for response not starting for values of the control signal below some threshold (25% for the cooling coil in the laboratory apparatus). As with Training 1, the model could be divided into two regions, the first below the threshold in which there is no response of the device (valve for Training 3) and the second in which the model can be expressed as a polynomial regression on the training data collected.

Completion of Full Suite of Laboratory Tests

Table 6 (in Chapter 3) identifies the faults for which algorithms were developed and software code implemented. Testing was completed for only a subset of the algorithms in this project, as reported in Table 7. A much more complete set of testing is required both to adjust the values of parameters for which values are selectable (e.g., the supply-fan control signal, $U_{SF,tol}$) and to validate all the algorithms. Furthermore, it is important to ensure that the fault detection and isolation algorithms can distinguish among different faults and not falsely isolate incorrect

faults. This will require testing the algorithms with many different faults, even those which are not correctable, as part of ensuring that false positive fault detection and incorrect fault isolation are minimized. Table 8 provides a list of all detectable VAV system faults identified in this project. Many of these faults would be trivial to detect, but the algorithms for their detection have not been coded in software yet to enable testing. Most of these faults are not self-correctable. Nevertheless, demonstrating that all faults can be successfully distinguished from one another is important. A key goal of the self-correcting controls process is not to "fix" faults that don't exist, which requires minimization of false positive fault detection and errors in fault isolation. Beyond proving this ability, performing tests on all of the faults will reveal weaknesses in the algorithms, which can then be used to formulate important improvements.

Table 10: Testing Status for all Faults in Filter/Fan/Coil and VAV-Box Sections of VAV Systems

Type of Fault	Fault Tested?	Comments
Hunting CC valve	No	
HC/CC valve controller software logic fault	No	
Fan controller software logic fault	No	
Supply-air flow station complete failure	No	
Supply-air fan complete failure	No	
Supply-air fan belt slipping/decreased fan η	No	
Supply-air flow station biased	Yes	
Supply-air flow station erratic	No	
CC valve stuck open or leaking	No	
HC valve stuck open or leaking	N/A	No heating coil in lab apparatus
MA temperature sensor biased	Yes	Tested in mixing-box tests (see Fernandez et al. 2009b)
MA temperature sensor erratic/not working	No	
HC temperature sensor biased	N/A	No heating coil in lab apparatus
HC temperature sensor erratic/not working	N/A	
SA temperature sensor biased	Yes	Algorithms working well
SA temperature sensor erratic/not working	No	
Filter is clogged/oversized	No	
Filter differential pressure sensor biased/ erratic/not working	No	

Type of Fault	Fault Tested?	Comments
Filter has fallen down or is installed incorrectly	No	
VAV box damper does not modulate in upper half of signal range	No	
VAV box damper does not modulate in lower half of signal range	No	
VAV box flow sensor is biased	No	
VAV box reheat coil valve stuck open or leaking	No	
Discharge air temperature sensor biased	No	
Discharge air temperature sensor erratic/not working	No	
VAV box flow station erratic/ not working	No	
VAV box damper stuck	No	
VAV box incorrect maximum flow set point	No	

Integrating with Additional BASs and Field Testing

Although the self-correcting control algorithms should be compatible with any building automation system, the linkages may vary from one BAS to another. Therefore, to ensure compatibility with the variety of BASs found in commercial buildings, the algorithms should be connected to and laboratory tested with BASs other than the Johnson Controls Metasys system used in the laboratory apparatus. The PNNL laboratory has the capability for such testing and will provide a suitable environment for such testing.

Field testing frequently identifies needs and issues not anticipated during initial development and laboratory testing. In preparation for commercial application, tests of the self-correcting control algorithms should be performed in operating commercial buildings to ensure compatibility with actual conditions in the field.

Path Forward

Given the status of the algorithms and testing, additional algorithm development and testing is clearly needed; however, even in the current state, a practical self-correcting control capability could be moved to field testing and commercial use relatively soon. The current plans of the PNNL project team, in addition to furthering development and testing, are to develop a field deployable, user compatible, software module for fault detection, isolation and correction for mixing-box sensors of air handlers. These algorithms have proven to perform well in

laboratory tests and, therefore, with limited additional laboratory testing, could be moved to field use. The team anticipates applying software for this purpose first to built-up air handlers (rather than air handling in packaged rooftop HVAC units).

As field test results provide data on the field performance of the algorithms and software as well as the prevalence and incidence of faults in the field, that information will be used to update the assessment of economic, energy and power demand impacts.

REFERENCES

Bass, F.M. 1969. "A New Product Growth Model for Consumer Durables." *Management Science,* Vol. 15 (5): pp. 215-227, January 1969.

Brown, M.A., L.G. Berry, and R.K. Goel. 1989. *Commercializing Government-Sponsored Innovations:*

Brown, M.A., L.G. Bery, R.A. Balzer, E. Faby. 1993. *National Impacts of the Weatherization Assistance Program in Single-Family and Small Multifamily Dwellings*. ORNL/CON-326. Oak Ridge National Laboratory, Oak Ridge, Tennessee.

California Energy Commission (CEC) 2009. *California Energy Demand 2010-2020 Adopted Forecast*. CEC-200-2009-012-CMF, California Energy Commission, Sacramento, California.

Dexter, A. and J. Pakanen, eds. 2001. *Demonstrating automated fault detection and diagnosis methods in real buildings*. International Energy Agency Annex 34, Technical Research Centre of Finland, Espoo, Finland.

Elliott DB, DM Anderson, DB Belzer, KA Cort, JA Dirks, and DJ Hostick. 2004. *Methodological Framework for Analysis of Building-Related Programs: The GPRA Metrics Effort, June 2004*. PNNL-14696, Pacific Northwest National Laboratory, Richland, WA. Available at: http://www.pnl.gov/main/publications/external/technical_reports/PNNL-14696.pdf.

Energy Information Administration (EIA). 2003. *Commercial Building Energy Use Survey* (CBECS) 2003. U.S. Department of Energy. Washington, D.C.

Energy Information Administration (EIA). 2010. *Annual Energy Outlook 2009*. U.S. Department of Energy, Washington, D.C.

Fernandez, N., S. Li, W. Wang and M.R. Brambley (Pacific Northwest National Laboratory). 2011. Self-*Correcting Controls for Variable Air Volume (VAV) Systems: Filter/Coil/Fan and VAV Box Sections*, California Energy Commission. Publication number: CEC-XXX-2011-XXX.

Fernandez, N., M.R. Brambley and S. Katipamula. 2009a. *Self-Correcting HVAC Controls: Algorithms for Sensors and Dampers in Air-Handling Units*, PNNL-19104. Pacific Northwest National Laboratory, Richland, WA.

Fernandez, N., M.R. Brambley, S. Katipamula, H. Cho, J. Goddard and L. Dinh. 2009b. *Self-Correcting HVAC Controls Project Final Report*, PNNL-19074. Pacific Northwest National Laboratory, Richland, WA.

Hyvarinen, J. and S. Karki, eds. 1996. *Building Optimization and Fault Diagnosis Source Book*. International Energy Agency Annex 25, Technical Research Center of Finland, Espoo, Finaland.

Itron, Inc. 2006. *California Commercial End-Use Survey*. Survey conducted for California Energy Commission. Publication # CEC-400-2006-005, March 2006.

Mahajan, V., C. Mason, and V. Srinivasan. 1986. "An Evaluation of Estimation Procedures for New Product Diffusion Models." In *Innovation Diffusion Models of New Product Acceptance*, V. Mahajan and Y. Wind, eds., Ballinger, Cambridge, Massachusetts.

Mills, Evan. 2009. *A Golden Opportunity for Reducing Energy Costs and Greenhouse Gas Emissions.* Lawrence Berkeley National Laboratory, Berkeley, Caifornia. Available online at: http://cx.lbl.gov/2009-assessment.html.

Moore, E., E. Crowe, A. Robbins and B. Walker. Portland Energy Conservation (PECI). 2008. "Making the Leap: Data and Lessons Learned from Scaling Up Retrocommissioning Programs." In Proceedings of the 2008 ACEEE Summer Study on Energy Efficiency in Buildings, pp. 4-230 – 4-242, American Council for an Energy Efficient Economy, Washington, D.C.

Northwest Energy Efficiency Alliance (NEEA). 2005. *Light Commercial HVAC.* Prepared by: Energy and Environmental Analysis. Report #E205-143. Northwest Energy Efficiency Alliance, Portland, OR.

Pacific Northwest National Laboratory (PNNL). 2008. *Facility Energy Decision System User's Guide, Release 6.0*. PNNL-17848, Pacific Northwest National Laboratory, Richland, Washington.

Roth, K.W., D. Westphalen, M.Y. Feng, P. Llana and L. Quartararo. 2005. *Energy Impact of commercial Building controls and Performance Diagnostics: Market characterization, Energy Impact of Building Faults and Energy Savings Potential.* Reference No. 02140-2390, TIAX, Lexington, Massachusetts. Prepared for the U.S. Department of Energy, Washington, D.C.

Smith, V.A. and Bushby, S. 2003. *Air Handling Unit and Variable Air Volume Box Diagnostics*, Technical Report P-500-03-096-A3, California Energy Commission, Sacramento, California.

Srinivasan, V. and C. Mason 1986. "Nonlinear Least Squares Estimation of New Product Diffusion Models," *Marketing Science.* 5 (Spring):169-78.

Tso, Bing, Nick Hall, Peter Lai, and Richard Pulliam. 2007. "How Much Does Retrocommissioning Really Save? Results From Three Commissioning Program Evaluations in California." In *Proceedings from the 2007 International Energy Program Evaluation Conference, Chicago*, 170-181. International Energy Program Evaluation Conference, Chicago, IL.

Twelve Successful Buildings Case Studies. ORNL/CON-275, Oak Ridge National Laboratory, Oak Ridge, Tennessee.

U.S. Environmental Protection Agency (EPA) 2007. "EPA's Emissions & Generation Resource Integrated Database (eGRID): Power Profiler eGRID subregion and GHG emissions finder tool." Washington, D.C. Located online: http://www.epa.gov/cleanenergy/energy-and-you/how-clean.html.